Original research

Refining nosology by modelling variation among facial phenotypes: the RASopathies

Harold Matthews ,[1,2,3] Michiel Vanneste,[1,2] Kaitlin Katsura,[4] David Aponte,[5] Michael Patton,[6] Peter Hammond,[1] Gareth Baynam,[7,8,9,10] Richard Spritz,[11] Ophir D Klein,[4] Benedikt Hallgrimsson,[5] Hilde Peeters,[1] Peter Claes[1,2,3,12]

► Additional supplemental material is published online only. To view, please visit the journal online (http://dx.doi.org/10.1136/jmedgenet-2021-108366).

For numbered affiliations see end of article.

Correspondence to
Professor Peter Claes, Medical Imaging Research Center, UZ Leuven, Leuven, Belgium; peter.claes@kuleuven.be

Received 6 December 2021
Accepted 18 May 2022

To cite: Matthews H, Vanneste M, Katsura K, *et al*. *J Med Genet* Epub ahead of print: [please include Day Month Year]. doi:10.1136/jmedgenet-2021-108366

ABSTRACT

Background In clinical genetics, establishing an accurate nosology requires analysis of variations in both aetiology and the resulting phenotypes. At the phenotypic level, recognising typical facial gestalts has long supported clinical and molecular diagnosis; however, the objective analysis of facial phenotypic variation remains underdeveloped. In this work, we propose exploratory strategies for assessing facial phenotypic variation within and among clinical and molecular disease entities and deploy these techniques on cross-sectional samples of four RASopathies: Costello syndrome (CS), Noonan syndrome (NS), cardiofaciocutaneous syndrome (CFC) and neurofibromatosis type 1 (NF1).

Methods From three-dimensional dense surface scans, we model the typical phenotypes of the four RASopathies as average 'facial signatures' and assess individual variation in terms of direction (what parts of the face are affected and in what ways) and severity of the facial effects. We also derive a metric of phenotypic agreement between the syndromes and a metric of differences in severity along similar phenotypes.

Results CFC shows a relatively consistent facial phenotype in terms of both direction and severity that is similar to CS and NS, consistent with the known difficulty in discriminating CFC from NS based on the face. CS shows a consistent directional phenotype that varies in severity. Although NF1 is highly variable, on average, it shows a similar phenotype to CS.

Conclusions We established an approach that can be used in the future to quantify variations in facial phenotypes between and within clinical and molecular diagnoses to objectively define and support clinical nosologies.

WHAT IS ALREADY KNOWN ON THIS TOPIC

⇒ Nosology in clinical genetics requires consideration of both aetiology and the resulting phenotype. While next-generation sequencing has advanced our understanding of the aetiology of many genetic conditions, methods for analysing facial phenotypic variation are underdeveloped.

WHAT THIS STUDY ADDS

⇒ This study describes a method for analysing variation in the facial phenotype within and among related conditions and applies the methods to samples of four RASopathies: Costello syndrome, Noonan syndrome, cardiofaciocutaneous syndrome and neurofibromatosis type 1.

HOW THIS STUDY MIGHT AFFECT RESEARCH, PRACTICE AND/OR POLICY

⇒ This study facilitates the objective study of variation in facial phenotypes with a view to the development of more objective nosologies in clinical genetics.

INTRODUCTION

Nosology concerns the definition and delineation of diseases. It requires a balance between 'lumping' similar diseases together and 'splitting' others into separate entities.[1] In clinical genetics, this process requires consideration of both aetiology and the resulting phenotype.[2] At the aetiological level, next-generation sequencing has greatly informed our understanding of the genetics underlying many syndromes. This includes genotype-first approaches, which have revealed that many monogenic syndromes, previously thought to be well defined, exhibit a much broader phenotypic spectrum than previously realised.[3 4] These findings have forced the definitions of certain syndromes and syndrome families to be revised.[5–7]

At the phenotypic level, inter-syndrome and intra-syndrome variation can be difficult to define objectively. Facial phenotyping in clinical genetics usually relies on recognition of a facial gestalt that is considered typical for a given clinical or molecular diagnosis and the translation of observations into standardised terminology.[8] In recent years, this has been augmented with computer software, such as 'Face2Gene',[9 10] for automated recognition of facial gestalts typical of various syndromes. Nevertheless, recognising facial gestalts does not yield straightforward measures of phenotypic variation and similarity. So-called 'clinical face phenotype spaces'[11 12] are high-dimensional spaces derived from patient images, wherein distances correspond to facial similarities such that similar patients and phenotypically similar disorders are positioned together. Despite the potential to inform nosological discussions, it remains unclear how phenotypic variation and similarity should be assessed within such a space. Different molecular or clinical entities can exhibit similar facial changes to the same parts of the face, but with different severity.[13] Alternatively, different parts of the face may be affected, or the same parts may be affected in different ways. In this work, we develop an exploratory strategy for

quantitatively describing the variation within, and similarities and differences among, facial phenotypes using dense three-dimensional (3D) surface scans. We deploy this approach to analyse four RASopathies. RASopathies are a family of well-studied disorders of the RAS/MAPK pathway, comprising Costello syndrome (CS), Noonan syndrome (NS), cardiofaciocutaneous syndrome (CFC) and neurofibromatosis type I (NF1), among others. Facial similarity and variation are well-understood clinically within this family of disorders, making them an interesting test case for the proposed methodology.

MATERIALS AND METHODS

Sample

The RASopathy patient sample is derived from three established resources: (1) the FaceBase repository (www.facebase.org; FB00000861)[14] ; (2) the database of the Western Australian Health Department; and (3) Peter Hammond's legacy 3D dysmorphology dataset hosted at KU Leuven, Belgium. Data ascertainment is described in online supplemental text 1. The study used all available data after excluding participants who: (1) had no image of acceptable quality; (2) did not have necessary demographic data (age, sex and ancestry) reported; (3) failed image registration (see further); (4) were a second image of a patient already included in the analysis; or (5) were of non-European ancestry. This last criterion was applied because each patient was assessed relative to an openly available normative reference for 3D facial shape (see further), which is based only on participants of European ancestry. The final dataset comprised patients with a diagnosis of NS (n=129; 57 female), NF1 (n=42; 23 female), CFC (n=51, 28 female) or CS (n=46; 30 female). Online supplemental table 1 shows numbers of participants remaining after each exclusion criterion was applied. Figure 1 illustrates the final dataset broken down by age, sex, clinical diagnosis and molecular diagnosis at the level of the affected gene. Online supplemental table 2 reports further details of the molecular diagnosis per participant.

Image preprocessing

Image processing

To obtain standard facial representations, each 3D facial photograph was non-rigidly registered with a standard template using the 'MeshMonk' MATLAB toolbox,[15 16] resulting in a representation of each face as a standard set of 7160 points. Images were visually inspected and were excluded if the registration had failed.

Each standardised point configuration was then converted into a 'facial signature',[17] which codes the deviations of each point on each patient from an age and sex matched normative reference face as z-scores. This essentially removes variation due to normal growth and sex differences on the face. This was done using the open-source 3D Growth Curves and Facial Assessment Toolbox in MATLAB, a normative reference for 3D facial shape based on a sample with European ancestry.[18] Facial signatures were calculated along the x (lateral–medial), y (inferior–superior) and z (anterior–posterior) direction as well as the direction normal to the facial surface at each quasilandmark. Facial signatures in the x, y and z directions were concatenated to define a single feature vector for each patient, which was used for all subsequent computation. These procedures essentially define a position for each patient in a high-dimensional space where each element of the feature vector is an axis and distance corresponds to facial similarity. The signatures along the surface normal were only used in visualisations. Furthermore, for visualisation, an age-normalised and sex-normalised facial shape of each patient was created by subtracting the coordinates of the age-and-sex-specific expected face from the coordinates of the patient and adding back on the coordinates of the overall average face of the 3D Growth Curve training data.

Assessing phenotypic consistency within the RASopathies

We assessed phenotypic consistency in terms of variation in direction (what parts of the face are affected and in what ways) and severity (to what degree is the face affected in a manner that is typical of the syndrome). The foregoing calculations can be interpreted geometrically as illustrated in figure 2. The aggregate phenotype of each RASopathy was defined as the mean feature vector (mean signature) of all patients with the syndrome. Directional similarity of the *i*th individual to the *j*th syndrome mean signature was calculated as the cosine distance between the individual and group mean feature vector:

$$x_{ij} = 1 - \frac{a_i \cdot \mu_j}{\|a_i\| \cdot \|\mu_j\|}$$

where a_i is the feature vector of the individual and μ_j is the average feature vector of the *j*th syndrome. This defined the typical phenotype of each syndrome as a transformation away from normal. Geometrically speaking, this was a direction or vector and similarity to it was measured as an angle (figure 2). Anatomically, an example direction might, for instance, be loosely verbally described as the distance between the eyes widening in conjunction with a shrinking chin. Patients displaying this pattern (irrespective of severity) will have a small cosine distance to the mean. In the example, a patient with severe hypertelorism and micrognathia will have a low cosine distance, as will a patient with less severe hypertelorism and micrognathia, as well as a patient that is within normal range but has relatively widely spaced eyes and a small chin. A patient with the inverse difference (eg, hypotelorism and macrognathia) will have a high cosine distance. The cosine distance is readily interpretable as it is on a normalised scale from 0 to 2. Values greater than 1 indicate the patient is better described displaying the inverse of the typical pattern than the typical pattern.

For the *i*th individual, their severity on the *j*th mean signature was:

$$p_{ij} = \frac{a_i \cdot \mu_j}{\|\mu_j\|}$$

Geometrically, this was a projection onto the average signature and was a scalar measure of the magnitude of the facial effect in the direction of the average signature. In the example introduced previously, a patient with more extreme micrognathia and hypertelorism will have a higher severity score than one with these features to a lesser degree. Variation in direction within a syndrome was measured as the root mean squared cosine distance from their average signature; we call this the 'directional variation statistic'. Variation in severity was measured by the standard deviation (SD) of their severity scores; we call this the 'severity variation statistic'.

Assessing phenotypic variation among the RASopathies

Two clinical or molecular entities may drive variation along similar or different directions. We assess this for each pair of disorders using the cosine of the angle between the mean signatures of the two disorders μ_i and μ_j:

$$c_{ij} = \frac{\mu_i \cdot \mu_j}{\|\mu_i\| \cdot \|\mu_j\|}$$

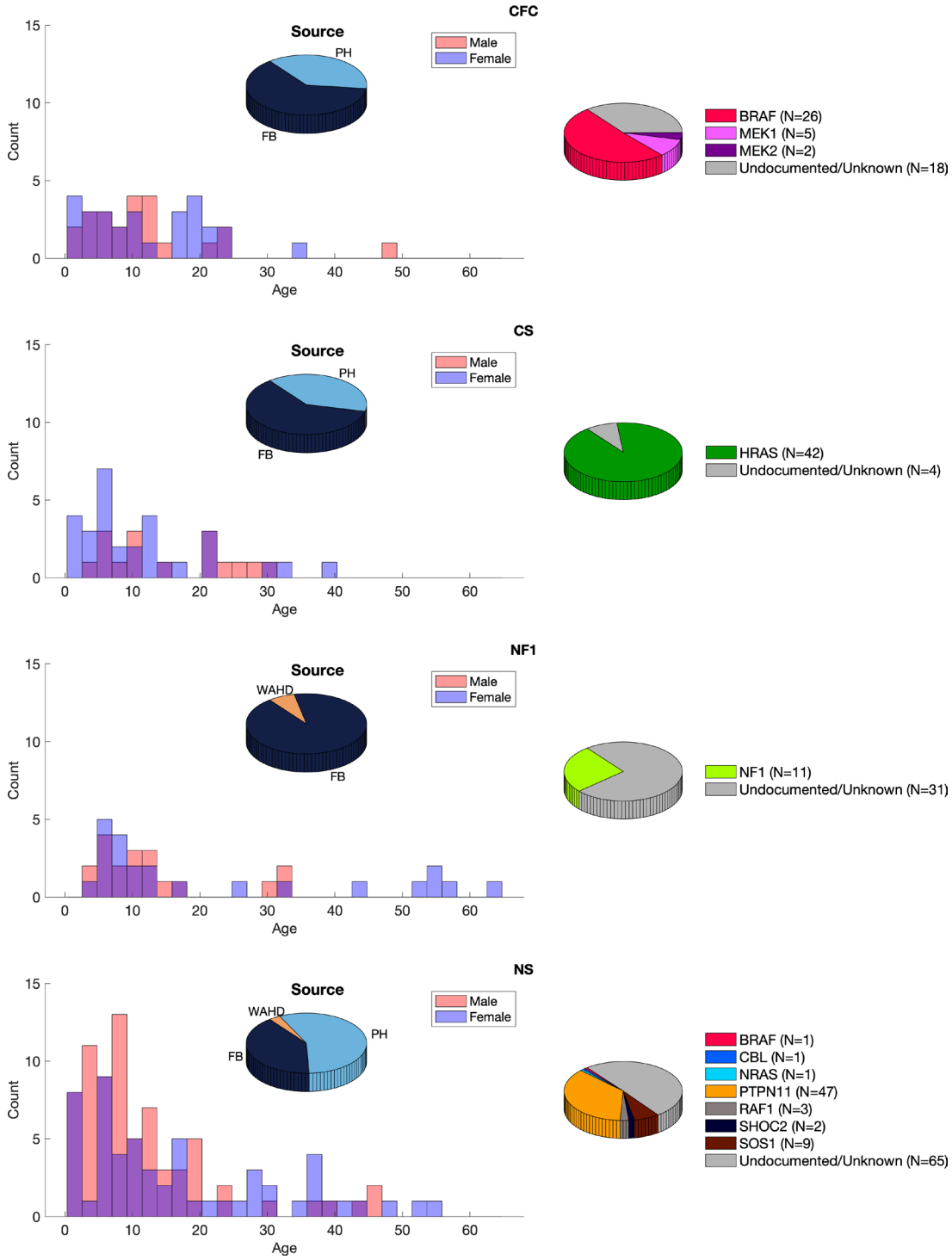

Figure 1 The RASopathy sample. Left shows the distribution of ages for each sex per group and the proportion of subjects coming from each of the three databases. Right shows numbers of molecularly confirmed (broken down by the affected gene) and unconfirmed cases. FB: the FaceBase repository; PH: Peter Hammond's legacy three-dimensional dysmorphology collection; WAHD: the Western Australian Department of Health.

We call this this the 'phenotype agreement score'. This ranges from 1 indicating the two signatures point in the same direction to −1, indicating the two signatures point in opposite directions.

Clinical or molecular disease entities may produce similar directional phenotypes but differ in severity. Therefore, we suggest a complementary measure: the 'severity difference score'. For each pair of syndromes, we compute the mean of the two average signatures and compute the severity scores of patients along this combined phenotype. We then compare the distributions of severity scores between the two syndromes using Cohen's d statistic, which is the difference between the syndrome means divided by the average of the SD of the two groups. Throughout, we use a leave-one-out approach, where the patient being scored is excluded from the estimation of the average signature. To estimate CIs of each statistic observations within each syndrome were randomly resampled 1000 times and the cosine distances, severity and derived statistics were recalculated.

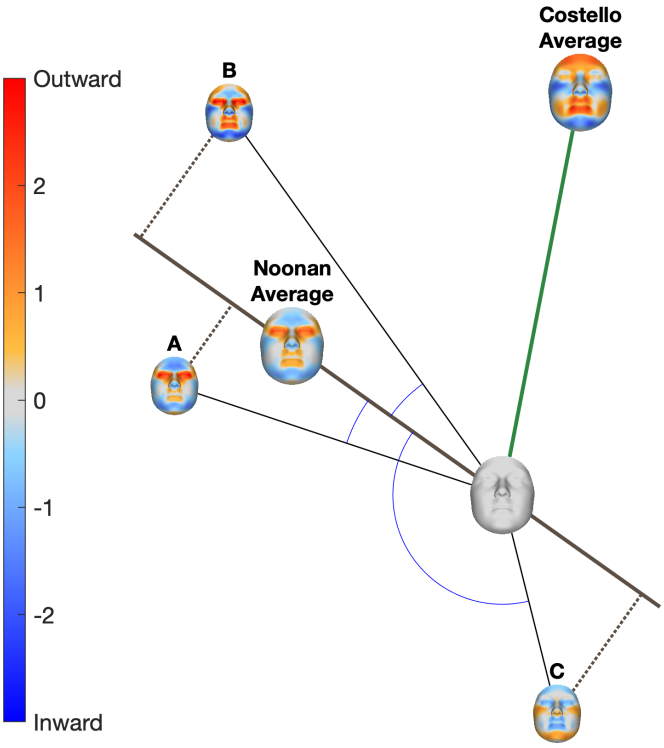

Figure 2 Description of cosine distance and severity measures. Each patient (A, B and C) is represented by their facial signature. The facial signature is shown graphically as a colour-coded map where red indicates the point on the face of the patient is displaced outwardly relative to normal and blue indicates it is displaced inwardly. The average signatures of all patients with Noonan syndrome and all patients with Costello syndrome are shown by the larger colour maps. Geometrically, each signature can be interpreted as a vector. Anatomically each signature can be interpreted as a particular transformation of facial shape away from average (blank signature), for example, eyes widening (red) in combination with a shrinking (blue) chin. Similarity, in terms of what parts of the face are affected in what ways is measured by the angle between two vectors. For example, patients A and B have small angles (low cosine distance) to the Noonan phenotype, indicating they are affected in a way that is characteristic of Noonan syndrome.

Interpreting the magnitude of the statistics

To estimate what constitutes moderate, strong and very strong consistency, we computed the two variation statistics on a sample of 39 syndromes and craniofacial malformations. We defined values indicating 'moderate', 'strong' and 'very strong' consistency as those lower than the 20th, 10th and 5th percentiles, respectively, of the distributions of these statistics. Similarly, to determine what is a 'moderate', 'strong' or 'very strong' phenotype agreement or severity difference, we computed these statistics for all pairs of syndromes in the expanded dataset and used thresholds corresponding to the 80th, 90th and 95th percentiles, respectively. These thresholds are arbitrary but quite conservative compared with common guidelines for interpreting other effect sizes. For comparison commonly used thresholds for Cohen's d (small=0.3, mod=0.5, large=0.8) indicate the mean of the second sample is positioned at the 62nd, 69th, and 79th percentiles of the first sample, respectively. The data used are described in online supplemental table 3, and the distributions of the statistics are reported in online supplemental figure 1 and online supplemental table 4.

RESULTS

Average signatures

In this section, we assess the typical facial phenotypes of each RASopathy. Figure 3 illustrates the average signature of each of the RASopathies. The signatures in the left panel describe the transformation visually in the horizontal (blue indicates lateral displacement, red indicates medial displacement), vertical (blue indicates inferior displacement, red indicates superior displacement) and depth (blue indicates posterior displacement, red indicates anterior displacement) directions as well as the directions locally perpendicular to the surface (blue indicates locally inward displacement, red indicates locally outward displacement). Many dysmorphic features typically used in clinical genetics can be inferred from particular colour patterns in these signatures: anterior and locally outward displacement of the points on the lips is consistent with full lips; posterior and inward displacement of the zygomatic region is consistent with malar hypoplasia; superior and posterior displacement of the points of the nose is consistent with a short, depressed nose; and inward and posterior displacement of points on the chin, together with a medial displacement of the left and right sides of the chin, indicates a retruded chin and narrow jaw consistent with micrognathia. These four clinical features, while most pronounced in CS, are present to some degree in all four of the RASopathy syndromes. Anterior displacement of the forehead indicates forehead prominence, which occurs to differing degrees in CFC, CS and NF1. Complex changes in all three dimensions, although also coded in the facial signatures, are most easily visually appreciated by inspecting the average and exaggerated faces. For example, the eyes in CFC and NS are prominent and widespaced with downslanting palpebral fissures.

Phenotypic consistency within the RASopathies

In this section, we assess the consistency of the facial phenotypes displayed within the samples of each of the four RASopathies. As described in the Methods, similarity to the average signature and severity was measured for each individual. Kernel densities, fitted to the distributions of these statistics for each syndrome, are shown in figure 4A. Syndromes in which the face is typically affected in the same direction (the same facial features are transformed in the same way, though potentially to different degrees) will have generally low cosine distances. This is indicated by the central tendency of these distributions and is summarised for each syndrome in the directional variation statistic (figure 4B). Individuals may also vary in the degree of this transformation ('severity'), and syndromes may vary in how much individuals within the syndrome vary in severity. This is captured in the dispersion of the distributions of severity scores (figure 4A), which is measured for each syndrome in the severity variation statistic (figure 4B). The central tendency of the severity distributions also partially reflects the average magnitude of the effect on the face but only in the direction modelled by the average signature; for example, faces exhibiting an extreme phenotype that is dissimilar to the average signature could have a low severity score. To put the two variation statistics into context, the estimated cut-offs indicating moderate, strong and very strong consistency are plotted as vertical and horizontal lines on figure 4B. To visually illustrate the breadth of the phenotypes observed within each syndrome, figure 4C shows average faces and signatures of the five patients that are most and the five patients that are least similar to the average signature (left). The phenotypes in CS and CFC show moderate to strong consistency in direction. NS shows slightly lower consistency, and NF1

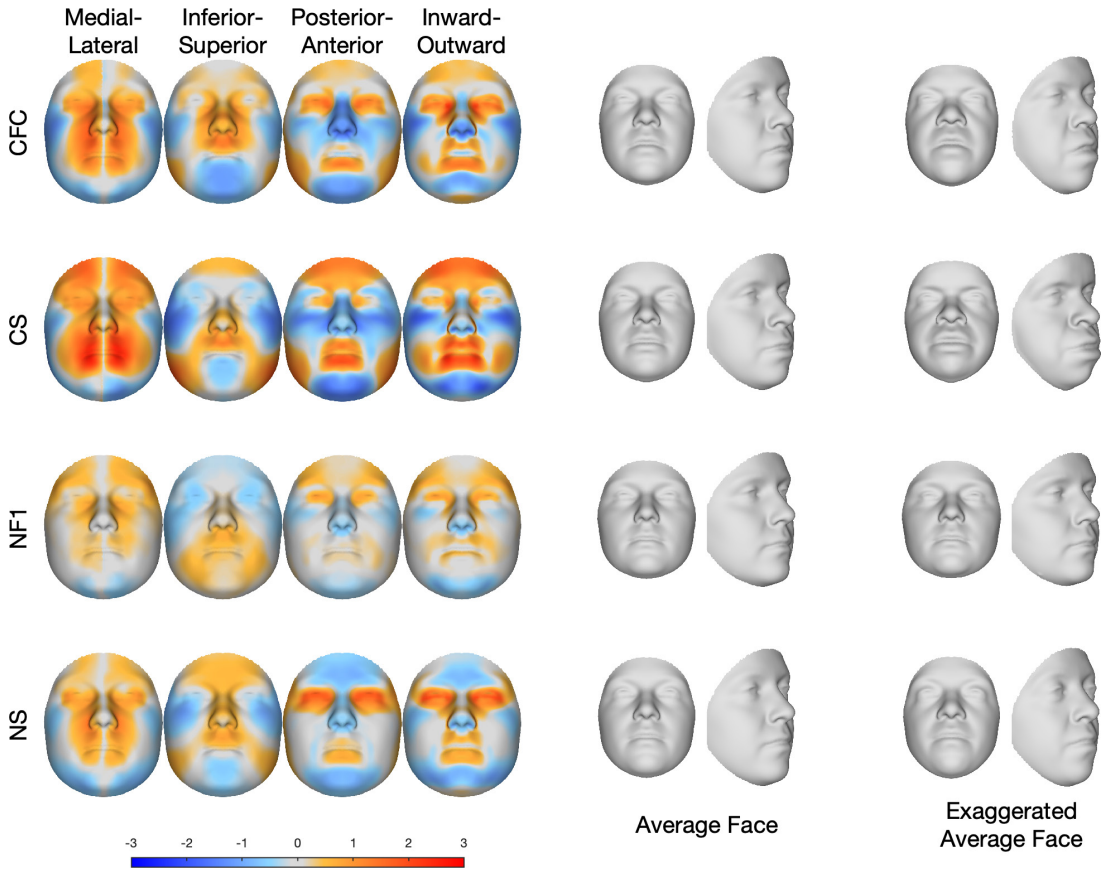

Figure 3 Average facial signatures in the horizontal direction (medial displacement=red; lateral displacement=blue); vertical direction (inferior displacement=blue, superior displacement=red); and depth (posterior displacement=blue, anterior displacement=red) and the direction locally perpendicular to the face (locally inward displacement=blue, locally outward displacement=red). The middle panel shows the average age and sex normalised face of each group, and the final panel shows an exaggerated version of the age and sex normalised average face.

shows very low consistency. CS and NF1 shows low consistency in severity, whereas CFC and NS are more consistent. This indicates that within CS and within CFC, and to a lesser extent within NS, the face is usually affected in similar directions (facial features are affected in similar ways). CS stands out because the direction of the effect is very consistent, though with variable severity (facial features may be affected to a greater or lesser degree). The phenotype of NF1 shows low consistency in terms of both direction and severity.

Phenotype agreement and severity differences among the RASopathies

In this section, we assess similarities and differences, in terms of direction and severity, among the RASopathy phenotypes. The relationship among the four syndrome phenotypes is summarised graphically in figure 5. Figure part A plots the phenotype agreement and severity difference statistics for each pair of syndromes. In terms of phenotype agreement, CFC is very strongly similar to NS and to CS, while CS is less similar (in the strongly–very strongly range) to NS. This indicates that CFC phenotype is intermediate between NS and CS. NF1 is very strongly similar to CS.

To assess differences in severity between two syndromes along a single direction, the average signatures of both syndromes were averaged, and the two groups were ordinated and compared along this combined signature. This assessment is less meaningful when there is less agreement between the average signatures of both groups. NF1 shows a strong to very strong severity difference to CS and CFC, with NF1 being less severe and is very strongly similar to CS. CFC paired with NS shows less than moderate severity difference, as does CFC paired with CS, CS paired with NS, and NF1 paired with NS.

The overall relationship among the average signatures is also approximated graphically on the first two axes of an uncentred principal components analysis of the average signatures and a signature that is all zeros (figure 5B). Here, the similarity between NF1 and CS is shown by their position along a similar vector from the origin, but at different distances, reflecting the difference in severity.

DISCUSSION

Over the past two decades, discovery of the molecular bases of many disorders has revealed unsuspected biological relationships among disorders that were previously thought to be unrelated.[4] At the same time, it has become clear that, for many Mendelian disorders, the range of associated phenotypes is considerably broader than was realised initially.[3 4] In many cases, this has resulted in substantial revision of syndrome nosology.[5–7] The recognition of typical facial gestalts has long supported clinical delineation of craniofacial syndromes. However, as the range of associated phenotypes for a given syndrome has broadened, the facial phenotypic gestalt often has become unclear.

Clinical face phenotype spaces (CFPSs)[11 12] position individuals within a continuous high-dimensional space, where informative image-based features, derived for all patients, are axes. Facially similar individuals and groups of individuals are

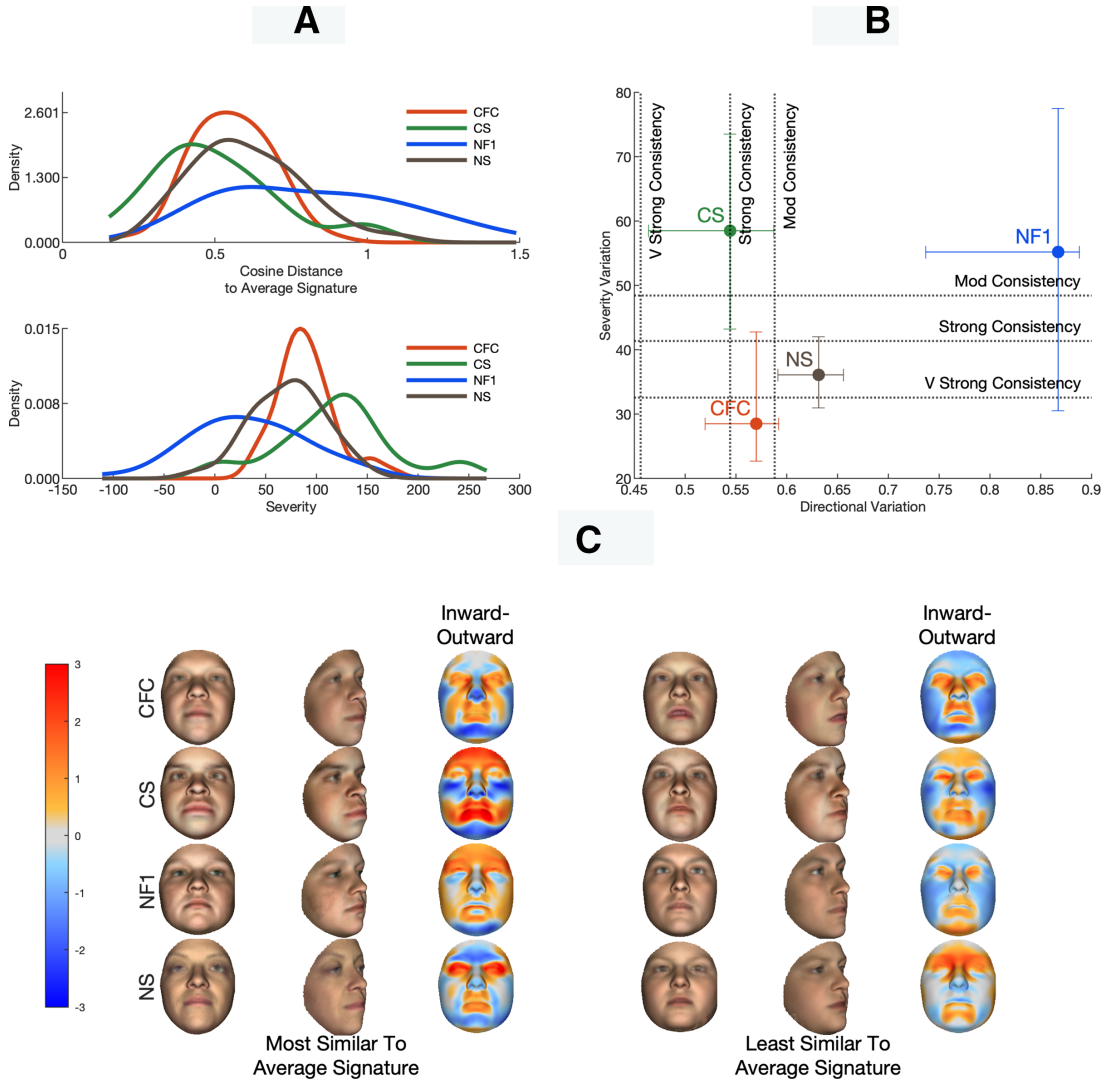

Figure 4 Consistency of the phenotypes of the four RASopathies. Figure part A plots fitted kernel densities to distributions of severity scores and cosine distance for each of the four syndromes. Figure part B plots the directional and severity variation statistics along with the defined cut-offs for mod, strong and very strong consistency. Error bars indicate the 95% CIs of the statistics estimated by resampling (see Materials and methods). Figure part C shows the average age-normalised and sex-normalised faces and of the five patients that are most and the five patients that are least similar (in terms of cosine distance) to the average signatures for each of the four groups as well as their average facial signatures, computed along the surface normals (red indicates locally outward displacement; blue indicates locally inward displacement).

positioned closely together in the space. Despite their potential for informing syndrome nosology, no established framework exists for establishing how syndromes are inter-related within such a space and how syndromes vary internally. In this work, we establish a CFPSfrom dense 3D surface scans, modelling variation in four RASopathies and develop a framework for exploring phenotypic variation within and among them.

An intuitively appealing approach to appreciate variation in a CFPS is to visualise the high-dimensional space as projections onto a low-dimensional space, via a dimension reduction technique such as principal components analysis,[19 20] t-distributed stochastic neighbour embedding[12 21] or signature graph analysis.[17] Any low-dimensional projection of a high-dimensional space will lose some aspects of the high-dimensional variation and a weakness of the aforementioned approaches is that the axes of the low-dimensional space are not necessarily biologically informative. Here, we began by modelling each syndrome group as a vector from average to the average signature of the syndrome. Projections onto this vector correspond to the degree to which an individual displays this combination of features. This differs from and complements other metrics of overall severity such as distance from the origin or the 'signature weight'[22] as it measures only variation that is most typical of the syndrome and has previously been shown to represent a biologically meaningful axis of 'severity'. For example, position along a similarly estimated axis was shown to correlate with the size of the causal deletion in Wolf-Hirschhorn syndrome.[13] The natural complement to this is angular variation with respect to the average signature vector, which corresponds to deviation from the typical facial transformation. To assess consistency of the facial phenotype, we use two univariate variation statistics based on angular similarity to and variation in the projection onto the average signature. These differ from other metrics of overall variation such as the trace of the within-class covariance matrix[23] in that they partition the variation into two separate components with different meanings. To investigate similarities and differences between facial phenotypes, we measure directional similarity between each pair of average signatures and differences in severity between each pair

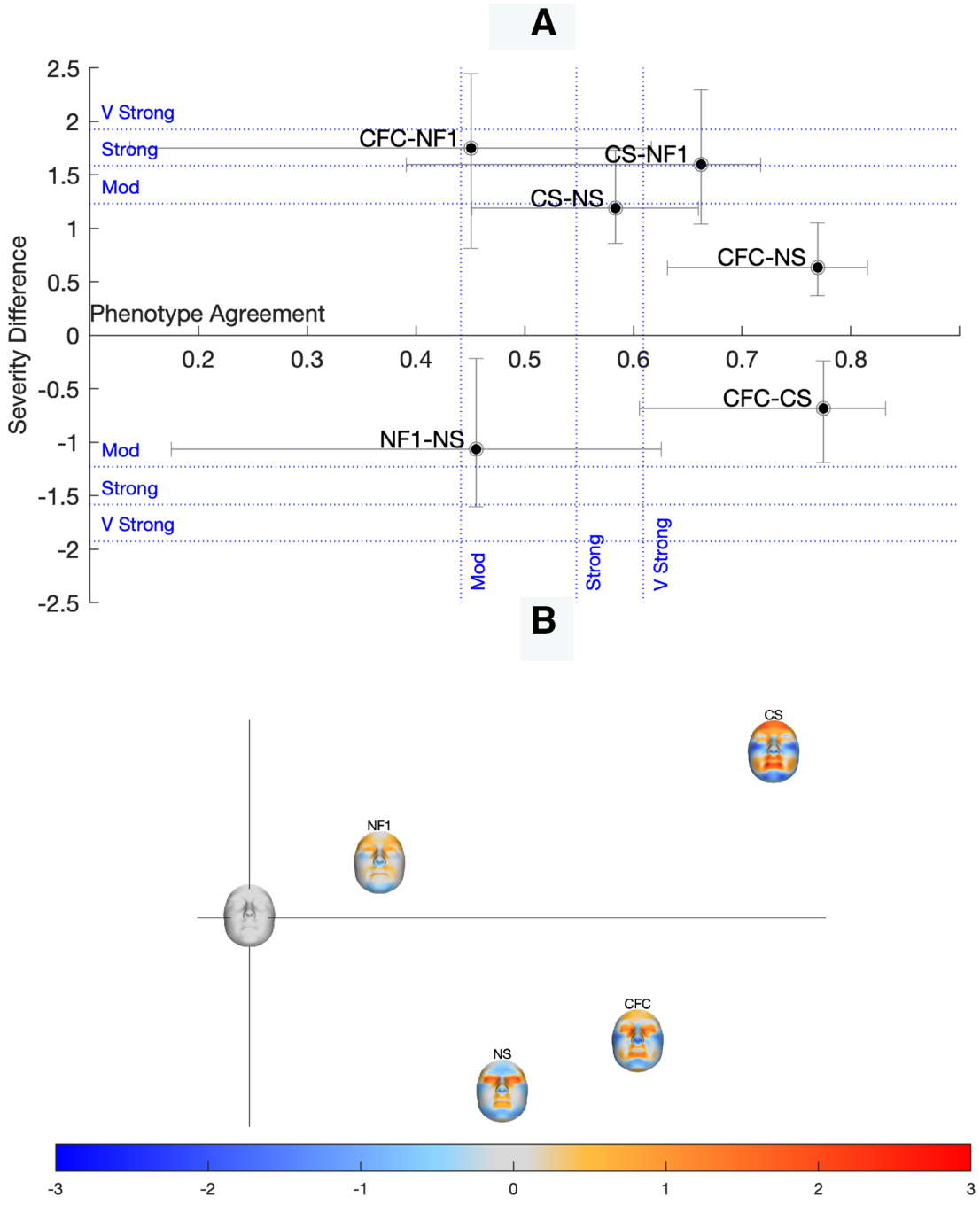

Figure 5 Phenotype agreement and severity difference among the RASopathies. Figure part A plots the phenotype agreement and severity difference statistics for each pair of RASopathies. The sign of the severity difference indicates whether the first syndrome was more severe than the second (positive) or the opposite (negative). Error bars indicate the 95% CIs of the statistics. Figure part B plots the average signatures on the first two principal components of an uncentred principal components analysis of the average signatures and a signature that is all zeros (the blank face at the origin). The facial signatures shown here are computed along the surface normals (red indicates locally outward displacement; blue indicates locally inward displacement).

of syndromes along a joint average signature. To interpret the magnitude of these statistics and to ascertain what are biologically meaningful values, we defined cut-offs based on distributions of similarly computed statistics from a larger sample of 39 genetic syndromes and craniofacial malformations. This constitutes a stronger approach than statistical hypthesis testing, which would only demostrate that the values of the statistics are non-zero in the population. However, this is limited by the particular constitution of this larger sample of syndromes, which cannot be assumed to be wholly representative of the population of all relevant conditions. Our particular choice of thresholds is conservative relative to most guidelines for interpreting effect sizes, although remains essentially arbitrary. More work is needed to understand fully how the magnitude of these statistics should be interpreted. Particularly how the variation statistics present in genetically homogeneous, as opposed to heterogeneous conditions can be investigated. Furthermore, it should be established how the statistics relate to measures of biological relatedness between syndromes, such as DNA methylation epi-signature similarity.[24]

While acknowledging the previous limitations, these statistics can be interpreted in combination to more fully assess phenotypic

variation among patient groupings, both within and between syndromes. Here we highlight some key findings in the context of clinical knowledge about the four RASopathies analysed in the study. CFC shows a relatively consistent phenotype in terms of both direction and severity. This is unexpected from a clinical point of view, as CFC is usually difficult to discriminate from CS and NS based on the face. This finding is more understandable when one also considers the phenotypic similarity among CS, CFC and NS. CFC is very strongly similar to CS and to NS. The average signatures illustrate that the phenotype of CFC entails a strong component of orbital hypertelorism as in NS while also displaying a more prominent forehead and full lips and cheeks, similar to CS. The face of CS is usually easy to recognise clinically, consistent with strong directional consistency of the phenotype, which comprises full-lips, malar hypoplasia, depressed nose, protruding forehead and retrognathia. More surprising is the low consistency (high variation) in severity for CS. As CS is genetically relatively homogeneous and is, with very few exceptions, caused by variants in the *HRAS* gene, the biological underpinnings of this variation are an important avenue for future research. NF1 shows a generally mild but highly variable phenotype in terms of both direction and severity, consistent with clinical lore that NF1 does not have a distinctive facial phenotype. Nevertheless, the average signature of NF1 is very strongly similar to that of CS, although with a strong severity difference between the two syndromes, indicating that the phenotype of NF1 is to some extent a milder version of that of CS. While some cases of NF1 have previously been found to be similar to NS,[25] the similarity between NF1 and NS is weaker than between NF1 and CS. Age-related changes to the statistics are investigated in online supplemental text 1. Directional variation declines with age for both NS and CS. CFC and CS increase in severity with increasing age, but variation in severity remains constant. Phenotype agreement between all pairs of syndromes, except NF1 paired with CS, declines with age. Severity difference increases with age for syndrome pairs CFC-NF1, CS-NF1 and NS-NF1.

The four RASopathies considered in this study are clinically defined entities that we treated as unified groups. It is possible that this may inflate variation and obscure interesting subtypes as these disorders are, to different degrees, genetically heterogeneous. CFC and NS can each be caused by variants in several genes including some genes (eg, *BRAF*) that can cause both. NF1 is caused exclusively by variants in the *NF1* gene; however, patients with microdeletions show relatively severe NF1 phenotypes.[26] CS is almost exclusively caused by a small number of variants affecting various codons in the *HRAS* gene. Analysis of molecularly defined categories is not feasible given the small sample sizes of patients with less common pathogenic variants available to us but is an important avenue for future work. Another possible effect of our reliance on clinical categorisation may be to reduce variation. In the absence of molecular confirmation, or in cases where the pathogenic variant does not uniquely specify the clinical diagnosis, the facial phenotype may have already been factored into the diagnosis. This could have reinforced the facial differences between the groups. This may be especially the case for NS and CS where the face is commonly used as part of diagnosis. This is likely to have had little influence on NF1 where the presence of particular facial features is not a diagnostic criterion.[27 28] Another possible impact of reliance on clinical diagnosis is the possible presence of misdiagnoses in the dataset, especially for patients where the diagnosis is not confirmed molecularly.

The application of next-generation sequencing in clinical genetics has rapidly expanded our understanding of the aetiology of many disorders; however, the complementary development of deep phenotyping technology has lagged far behind. Here, we have developed an approach to quantitatively measure both within and between-syndrome phenotypic variation, consistency and severity, and we apply these techniques to characterise both similarity and differences of both direction and severity. We applied these techniques to analyse a clinically well-studied group of related disorders characterised by variants in genes encoding protein components of the RAS/MAPK pathway, and we show how this approach can highlight phenotypic relationships among these related clinical entities. In the future, we anticipate that these techniques can contribute to developing a more objective nosology in clinical genetics.

Author affiliations
[1]Department of Human Genetics, KU Leuven, Leuven, Flemish Brabant, Belgium
[2]Medical Imaging Research Center, UZ Leuven, Leuven, Flemish Brabant, Belgium
[3]Facial Sciences Research Group, Murdoch Children's Research Institute, Parkville, Victoria, Australia
[4]Program in Craniofacial Biology, Departments of Orofacial Sciences and Pediatrics, and Institute for Human Genetics, University of California San Francisco, San Francisco, California, USA
[5]Department of Cell Biology and Anatomy, University of Calgary Cumming School of Medicine, Calgary, Alberta, Canada
[6]Medical Genetics Unit, St George's University of London, London, UK
[7]Western Australian Register of Developmental Anomalies, King Edward Memorial Hospital, Perth, Western Australia, Australia
[8]Telethon Kids Institute and Division of Paediatrics, Faculty of Health and Medical Sciences, The University of Western Australia, Perth, Western Australia, Australia
[9]School of Earth and Planetary Sciences, Faculty of Science and Engineering, Curtin University, Perth, Western Australia, Australia
[10]Faculty of Medicine, Notre Dame University, Fremantle, Western Australia, Australia
[11]Department of Paediatrics, University of Colorado Denver School of Medicine, Aurora, Colorado, USA
[12]Department of Electrical Engineering ESAT/PSI, KU Leuven, Leuven, Flemish Brabant, Belgium

Acknowledgements We acknowledge Professor Judith Allanson from the University of Ottawa and Professor Raoul Hennekam from the University of Amsterdam for their contributions to recruitment and data collection.

Contributors HM designed and implemented all analyses with input from PC and BH. HM wrote the first draft of the manuscript. MV, KK, DA, MP, PH, GB, RS, ODK, BH and HP revised the manuscript, providing insights on the clinical and biological context of the work. KK, DA, MP, PH, GB, RS, ODK and BH were responsible for data collection and recruitment. HM is responsible for the overall content as the guarantor.

Funding This work was supported by the research fund KU Leuven (BOF-C1, C14/15/081 & C14/20/081; PC); NIH-NIDCR (U01DE024440; RS, ODK and BH); the Research Programme of the Research Foundation Flanders (Belgium) (FWO, G078518N; PC). HP is a senior clinical investigator of the FWO (18B1521N).

Competing interests None declared.

Patient consent for publication Not applicable.

Ethics approval The study was approved by the ethical review board of KU Leuven and University Hospitals Gasthuisberg, Leuven (S56392). Patient recruitment and data collection at various centres was approved by: University College London Hospital (JREC00/E042); University of Calgary (REB14-0340); University of Colorado (14-0419); Stanford University (IRB-35709); University of Southern California (CCI-08-00150) University of California, San Francisco (14-12955); and the King Edward's Memorial Hospital (RGS0000002376; RGS0000002682). All analyses were carried out in accordance with the relevant guidelines and regulations. Participants gave informed consent to participate in the study before taking part.

Provenance and peer review Not commissioned; externally peer reviewed.

Data availability statement Data are available in a public, open access repository. The data from the FaceBase repository (https://doi.org/10.25550/1WWC) are available to researchers pending an approved data access request. Data from other sources were collected without approval for broad data sharing and are not publicly available.

ORCID iD
Harold Matthews http://orcid.org/0000-0002-0524-0025

REFERENCES

1 McKusick VA, Lumpers O. On Lumpers and splitters, or the nosology of genetic disease. *Perspect Biol Med* 1969;12:298–312.
2 Biesecker LG, Adam MP, Alkuraya FS, Amemiya AR, Bamshad MJ, Beck AE, Bennett JT, Bird LM, Carey JC, Chung B, Clark RD, Cox TC, Curry C, Dinulos MBP, Dobyns WB, Giampietro PF, Girisha KM, Glass IA, Graham JM, Gripp KW, Haldeman-Englert CR, Hall BD, Innes AM, Kalish JM, Keppler-Noreuil KM, Kosaki K, Kozel BA, Mirzaa GM, Mulvihill JJ, Nowaczyk MJM, Pagon RA, Retterer K, Rope AF, Sanchez-Lara PA, Seaver LH, Shieh JT, Slavotinek AM, Sobering AK, Stevens CA, Stevenson DA, Tan TY, Tan W-H, Tsai AC, Weaver DD, Williams MS, Zackai E, Zarate YA. A dyadic approach to the delineation of diagnostic entities in clinical genomics. *The American Journal of Human Genetics* 2021;108:8–15.
3 Bögershausen N, Wollnik B. Mutational landscapes and phenotypic spectrum of SWI/SNF-related intellectual disability disorders. *Front Mol Neurosci* 2018;11:252.
4 Kline AD, Moss JF, Selicorni A, Bisgaard A-M, Deardorff MA, Gillett PM, Ishman SL, Kerr LM, Levin AV, Mulder PA, Ramos FJ, Wierzba J, Ajmone PF, Axtell D, Blagowidow N, Cereda A, Costantino A, Cormier-Daire V, FitzPatrick D, Grados M, Groves L, Guthrie W, Huisman S, Kaiser FJ, Koekkoek G, Levis M, Mariani M, McCleery JP, Menke LA, Metrena A, O'Connor J, Oliver C, Pie J, Piening S, Potter CJ, Quaglio AL, Redeker E, Richman D, Rigamonti C, Shi A, Tümer Z, Van Balkom IDC, Hennekam RC. Diagnosis and management of Cornelia de Lange syndrome: first international consensus statement. *Nat Rev Genet* 2018;19:649–66.
5 Zhang LX, Lemire G, Gonzaga-Jauregui C, Molidperee S, Galaz-Montoya C, Liu DS, Verloes A, Shillington AG, Izumi K, Ritter AL, Keena B, Zackai E, Li D, Bhoj E, Tarpinian JM, Bedoukian E, Kukolich MK, Innes AM, Ediae GU, Sawyer SL, Nair KM, Soumya PC, Subbaraman KR, Probst FJ, Bassetti JA, Sutton RV, Gibbs RA, Brown C, Boone PM, Holm IA, Tartaglia M, Ferrero GB, Niceta M, Dentici ML, Radio FC, Keren B, Wells CF, Coubes C, Laquerrière A, Aziza J, Dubucs C, Nampoothiri S, Mowat D, Patel MS, Bracho A, Cammarata-Scalisi F, Gezdirici A, Fernandez-Jaen A, Hauser N, Zarate YA, Bosanko KA, Dieterich K, Carey JC, Chong JX, Nickerson DA, Bamshad MJ, Lee BH, Yang X-J, Lupski JR, Campeau PM. Further delineation of the clinical spectrum of KAT6B disorders and allelic series of pathogenic variants. *Genetics in Medicine* 2020;22:1338–47.
6 Bhoj EJ, Haye D, Toutain A, Bonneau D, Nielsen IK, Lund IB, Bogaard P, Leenskjold S, Karaer K, Wild KT, Grand KL, Astiazaran MC, Gonzalez-Nieto LA, Carvalho A, Lehalle D, Amudhavalli SM, Repnikova E, Saunders C, Thiffault I, Saadi I, Li D, Hakonarson H, Vial Y, Zackai E, Callier P, Drunat S, Verloes A. Phenotypic spectrum associated with SPECC1L pathogenic variants: new families and critical review of the nosology of Teebi, Opitz GBBB, and Baraitser-Winter syndromes. *Eur J Med Genet* 2019;62:103588.
7 Mortier GR, Cohn DH, Cormier-Daire V, Hall C, Krakow D, Mundlos S, Nishimura G, Robertson S, Sangiorgi L, Savarirayan R, Sillence D, Superti-Furga A, Unger S, Warman ML. Nosology and classification of genetic skeletal disorders: 2019 revision. *Am J Med Genet A* 2019;179:2393–419.
8 Carey JC. Special issue: elements of morphology: standard terminology. *Am J Med Genet* 2009;194A:1–127.
9 Gurovich Y, Hanani Y, Bar O, Nadav G, Fleischer N, Gelbman D, Basel-Salmon L, Krawitz PM, Kamphausen SB, Zenker M, Bird LM, Gripp KW. Identifying facial phenotypes of genetic disorders using deep learning. *Nat Med* 2019;25:60–4.
10 Latorre-Pellicer A, Ascaso Ángela, Trujillano L, Gil-Salvador M, Arnedo M, Lucia-Campos C, Antoñanzas-Pérez R, Marcos-Alcalde I, Parenti I, Bueno-Lozano G, Musio A, Puisac B, Kaiser FJ, Ramos FJ, Gómez-Puertas P, Pié J. Evaluating Face2Gene as a tool to identify Cornelia de Lange syndrome by facial phenotypes. *Int J Mol Sci* 2020;21:1042.
11 Ferry Q, Steinberg J, Webber C, FitzPatrick DR, Ponting CP, Zisserman A, Nellåker C. Diagnostically relevant facial gestalt information from ordinary photos. *eLife* 2014;3:e02020.
12 Hsieh T-C, Bar-Haim A, Moosa S, Ehmke N, Gripp KW, Pantel JT, Danyel M, Mensah MA, Horn D, Rosnev S, Fleischer N, Bonini G, Hustinx A, Schmid A, Knaus A, Javanmardi B, Klinkhammer H, Lesmann H, Sivalingam S, Kamphans T, Meiswinkel W, Ebstein F, Krüger E, Küry S, Bézieau S, Schmidt A, Peters S, Engels H, Mangold E, Kreiß M, Cremer K, Perne C, Betz RC, Bender T, Grundmann-Hauser K, Haack TB, Wagner M, Brunet T, Bentzen HB, Averdunk L, Coetzer KC, Lyon GJ, Spielmann M, Schaaf C, Mundlos S, Nöthen MM, Krawitz P. GestaltMatcher: overcoming the limits of rare disease matching using facial phenotypic descriptors. *medRxiv* 2021.
13 Hammond P, Hannes F, Suttie M, Devriendt K, Vermeesch JR, Faravelli F, Forzano F, Parekh S, Williams S, McMullan D, South ST, Carey JC, Quarrell O. Fine-grained facial phenotype-genotype analysis in Wolf-Hirschhorn syndrome. *Eur J Hum Genet* 2012;20:33–40.
14 Hallgrimsson B, Klein O, Spritz R. Developing 3D craniofacial morphometry data and tools to transform dysmorphology. *FaceBase* 2017.
15 White JD, Ortega-Castrillón A, Matthews H, Zaidi AA, Ekrami O, Snyders J, Fan Y, Penington T, Van Dongen S, Shriver MD, Claes P. MeshMonk: open-source large-scale intensive 3D phenotyping. *Sci Rep* 2019;9:6085.
16 Matthews HS, Burge JA, Verhelst P-JR, Politis C, Claes PD, Penington AJ. Pitfalls and promise of 3-dimensional image comparison for craniofacial surgical assessment. *Plast Reconstr Surg Glob Open* 2020;8:e2847.
17 Hammond P, Suttie M, Hennekam RC, Allanson J, Shore EM, Kaplan FS. The face signature of fibrodysplasia ossificans progressiva. *Am J Med Genet A* 2012;158A:1368–80.
18 Matthews HS, Palmer RL, Baynam GS, Quarrell OW, Klein OD, Spritz RA, Hennekam RC, Walsh S, Shriver M, Weinberg SM, Hallgrimsson B, Hammond P, Penington AJ, Peeters H, Claes PD. Large-Scale open-source three-dimensional growth curves for clinical facial assessment and objective description of facial dysmorphism. *Sci Rep* 2021;11:12175.
19 Jolliffe IT, Cadima J. Principal component analysis: a review and recent developments. *Philos Trans A Math Phys Eng Sci* 2016;374.
20 Mutsvangwa T, Douglas TS. Morphometric analysis of facial landmark data to characterize the facial phenotype associated with fetal alcohol syndrome. *J Anat* 2007;210:209–20.
21 van der Maaten L, Hinton G. Visualizing data using tSNE. *Mach Learn* 2008;9:2579–605.
22 Hammond P, Suttie M. Large-Scale objective phenotyping of 3D facial morphology. *Hum Mutat* 2012;33:817–25.
23 Hallgrímsson B, Aponte JD, Katz DC, Bannister JJ, Riccardi SL, Mahasuwan N, McInnes BL, Ferrara TM, Lipman DM, Neves AB, Spitzmacher JAJ, Larson JR, Bellus GA, Pham AM, Aboujaoude E, Benke TA, Chatfield KC, Davis SM, Elias ER, Enzenauer RW, French BM, Pickler LL, Shieh JTC, Slavotinek A, Harrop AR, Innes AM, McCandless SE, McCourt EA, Meeks NJL, Tartaglia NR, Tsai AC-H, Wyse JPH, Bernstein JA, Sanchez-Lara PA, Forkert ND, Bernier FP, Spritz RA, Klein OD. Automated syndrome diagnosis by three-dimensional facial imaging. *Genet Med* 2020;22:1682–93.
24 Aref-Eshghi E, Kerkhof J, Pedro VP, Barat-Houari M, Ruiz-Pallares N, Andrau J-C, Lacombe D, Van-Gils J, Fergelot P, Dubourg C, Cormier-Daire V, Rondeau S, Lecoquierre F, Saugier-Veber P, Nicolas G, Lesca G, Chatron N, Sanlaville D, Vitobello A, Faivre L, Thauvin-Robinet C, Laumonnier F, Raynaud M, Alders M, Mannens M, Henneman P, Hennekam RC, Velasco G, Francastel C, Ulveling D, Ciolfi A, Pizzi S, Tartaglia M, Heide S, Héron D, Mignot C, Keren B, Whalen S, Afenjar A, Bienvenu T, Campeau PM, Rousseau J, Levy MA, Brick L, Kozenko M, Balci TB, Siu VM, Stuart A, Kadour M, Masters J, Takano K, Kleefstra T, de Leeuw N, Field M, Shaw M, Gecz J, Ainsworth PJ, Lin H, Rodenhiser DI, Friez MJ, Tedder M, Lee JA, DuPont BR, Stevenson RE, Skinner SA, Schwartz CE, Genevieve D, Sadikovic B. Evaluation of DNA methylation Episignatures for diagnosis and phenotype correlations in 42 Mendelian neurodevelopmental disorders. *The American Journal of Human Genetics* 2020;106:356–70.
25 Denayer E, Legius E. Neurofibromatosis Type 1-Noonan Syndrome: What's the Link? In: *Noonan Syndrome and Related Disorders - A Matter of Deregulated Ras Signaling*. , 2009: 17, 128–37.
26 Serra G, Antona V, Corsello G, Zara F, Piro E, Falsaperla R. Nf1 microdeletion syndrome: case report of two new patients. *Ital J Pediatr* 2019;45:138.
27 Neurofibromatosis. Conference statement. National Institutes of health consensus development conference. *Arch Neurol* 1988;45:575–8.
28 Legius E, Messiaen L, Wolkenstein P, Pancza P, Avery RA, Berman Y, Blakeley J, Babovic-Vuksanovic D, Cunha KS, Ferner R, Fisher MJ, Friedman JM, Gutmann DH, Kehrer-Sawatzki H, Korf BR, Mautner V-F, Peltonen S, Rauen KA, Riccardi V, Schorry E, Stemmer-Rachamimov A, Stevenson DA, Tadini G, Ullrich NJ, Viskochil D, Wimmer K, Yohay K, Gomes A, Jordan JT, Mautner V, Merker VL, Smith MJ, Stevenson D, Anten M, Aylsworth A, Baralle D, Barbarot S, Barker F, Ben-Shachar S, Bergner A, Bessis D, Blanco I, Cassiman C, Ciavarelli P, Clementi M, Frébourg T, Giovannini M, Halliday D, Hammond C, Hanemann CO, Hanson H, Heiberg A, Joly P, Kalamarides M, Karajannis M, Kroshinsky D, Larralde M, Lázaro C, Le L, Link M, Listernick R, MacCollin M, Mallucci C, Moertel C, Mueller A, Ngeow J, Oostenbrink R, Packer R, Papi L, Parry A, Peltonen J, Pichard D, Poppe B, Rezende N, Rodrigues LO, Rosser T, Ruggieri M, Serra E, Steinke-Lange V, Stivaros SM, Taylor A, Toelen J, Tonsgard J, Trevisson E, Upadhyaya M, Varan A, Wilson M, Wu H, Zadeh G, Huson SM, Evans DG, Plotkin SR. Revised diagnostic criteria for neurofibromatosis type 1 and Legius syndrome: an international consensus recommendation. *Genet Med* 2021;23:1506–13.

Supplementary Text 1

1 Data Ascertainment

Patients from the FaceBase repository (collection: FB00000861) were recruited at patient meetings and genetics clinics in Colorado, Los Angeles, San Francisco, Stanford, USA and Alberta, Canada. If patients were recruited at a patient meeting, diagnosis was usually self-reported. When patients were seen at a clinic, a clinical diagnosis was established by a clinical geneticist, often followed by molecular confirmation. Patients in the database of the Western Australian Health Department were ascertained through multi-stakeholder (including patient) scientific meetings after individual in person review by a clinical geneticist (author GB) or via clinical geneticists directly from clinical genetics services. Patients in Peter Hammond's collection were recruited at patient support groups across the United States, UK and Italy. At initial recruitment, diagnosis was recorded as reported by families or suggested by clinical geneticists attending the meetings; some patients were in contact over several years and molecular diagnoses were reported by parents or by collaborating clinical geneticists.

2 Age-related changes to variation and similarity statistics

In the main text we use facial signatures to describe each patient. These represent how each patient differs from an age- and sex- appropriate normal reference population. Using facial signatures adjusts for the effects of normal growth and development on the face. However, age-related changes due to abnormal growth (such as the gradual appearance of syndrome-specific features) may still occur and these can affect the statistics presented in this paper. In this section we investigate these changes in the sample of RASopathies.

2.1 Age-related changes to directional variation

Directional variation is defined as the central tendency of the distribution of cosine distances from the mean signature. To investigate age-related changes to directional variation we regressed cosine distance to the mean signature onto age within each of the four syndromes. This was done using ordinary least-squares regression. The results are shown in Supplementary Text Figure 1. The regressions within CS and NS were significant suggesting that directional variation declines with age in these syndromes.

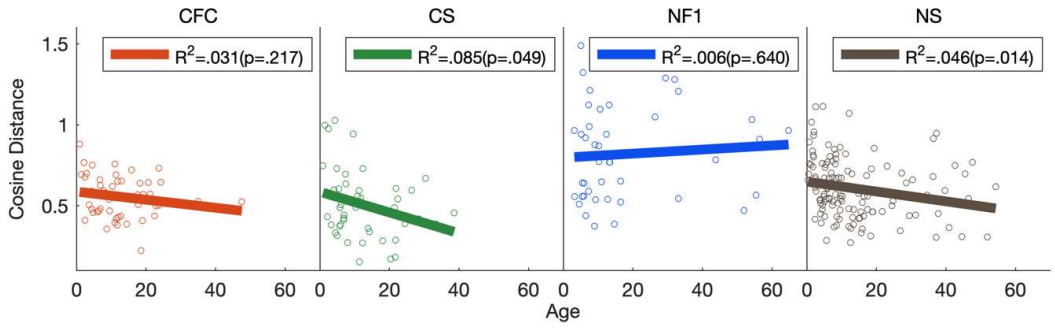

Supplementary Text Figure 1. Age-related changes to the directional variation statistic. In general cosine distance to the mean signature declines with age in CS and NS.

2.2 Age-related changes to severity and severity variation

We assessed age-related changes to severity via ordinary least-squares regression of severity onto age. Severity variation is the dispersion of severity scores from their central tendency. To assess age-related changes to severity variation we tested for changes to the dispersion relative to the linear regression (i.e. the dispersion of the residuals of the regression) using the Breusch-Pagan test for heteroscedasticity. Results are shown Supplementary Text Figure 2. CFC and CS become more severe with age. There is no evidence of heteroscedasticity for any of the syndromes and thus no evidence for age-related changes in severity variation.

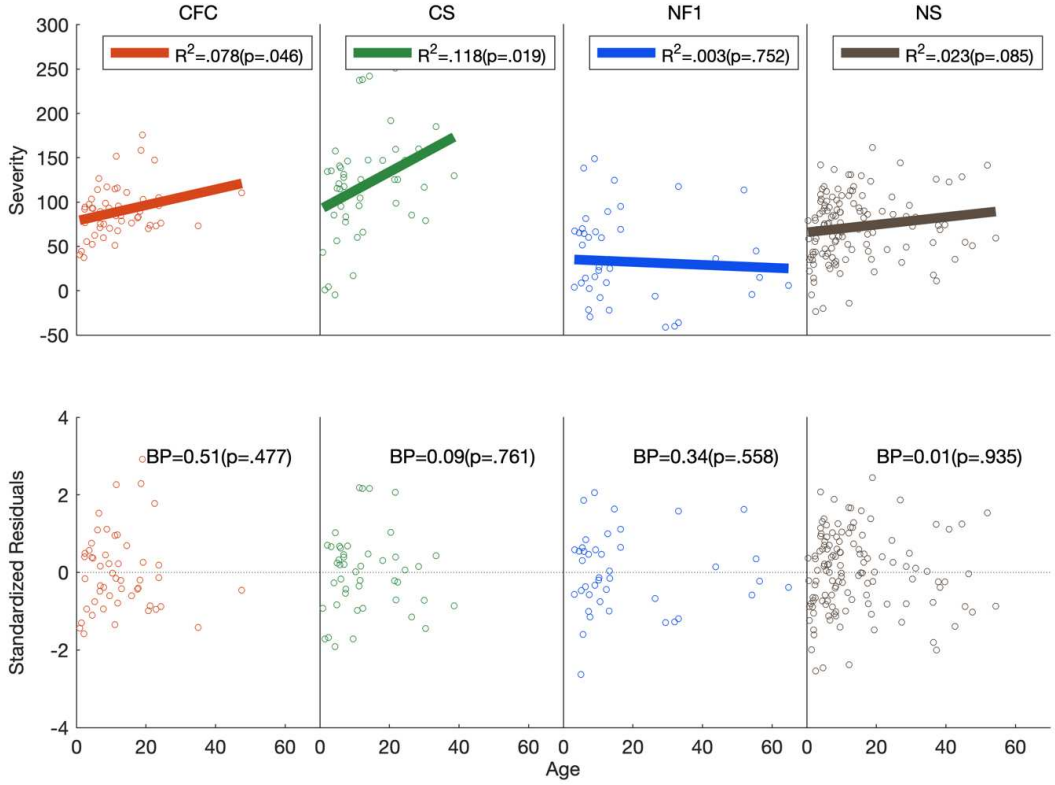

Supplementary Text Figure 2. Age-related changes in severity and severity variation. The top row plots the linear regression of severity onto age. CFC and CS become more severe with age. The bottom row plots the standardized residuals of each regression. BP denotes the Breusch-Pagan statistic.

2.3 Age-related changes to the typical phenotype and the phenotype agreement statistics

Age-related changes to phenotype agreement were assessed by firstly modelling the age-related change in the facial signatures for each syndrome. This was approximated using a multivariate linear partial least-squares regression of the signatures onto age. This fits the model:

$$\hat{Y} = MX + C$$

Where $\hat{Y}$ denotes the matrix of fitted values (expected signatures), M denotes the matrix of regression coefficients, X denotes the matrix of predictors (in this case only age), and C denotes the matrix of constant values. A model was fitted separately for each syndrome and statistical significance was evaluated using a permutation test on the variance explained (R^2) as per Shrimpton et al. [1]. The regressions were also evaluated at ages 5 and 50, yielding

expected signatures for each age for each syndrome. As these result from the imposition of a linear model, where changes would in fact be expected be non-linear, these should not be taken as exact age-specific estimates of the typical phenotype. Nevertheless, comparing the expected signatures at different ages can reveal the general trend of changes in the phenotype. For calculating phenotype agreement and statistical significance we used as signatures feature vectors combining signatures in the x y and z direction, as were used as the basis for all statistical analysis in this article. For illustrating the expected signatures we fitted separate models regressing the signatures in the direction normal to the surface onto age.

For illustration, the expected signatures in the direction normal to the surface are shown in Supplementary Text Figure 3 part (a). The regressions for CS (R^2=.070; p<.001) and NS (R^2=.020; p=.003) were significant. In general, the trend in CS is for features to become more extreme (the colors become deeper) consistent with the age-related change in severity observed in section 2.2 above. The submalar and mandibular portion of the cheeks also become less prominent (this region goes from being orange to light blue). In NS the prominence of the lips increases (this region becomes redder). The forehead and chin become bluer consistent with increased retrusion of the forehead and increased micrognathia. The middle malar and submalar regions of the cheeks become more prominent (redder). The regressions for CFC (R^2=.031; p=.109) and NF1 were non-significant (R^2=.019; p=.641).

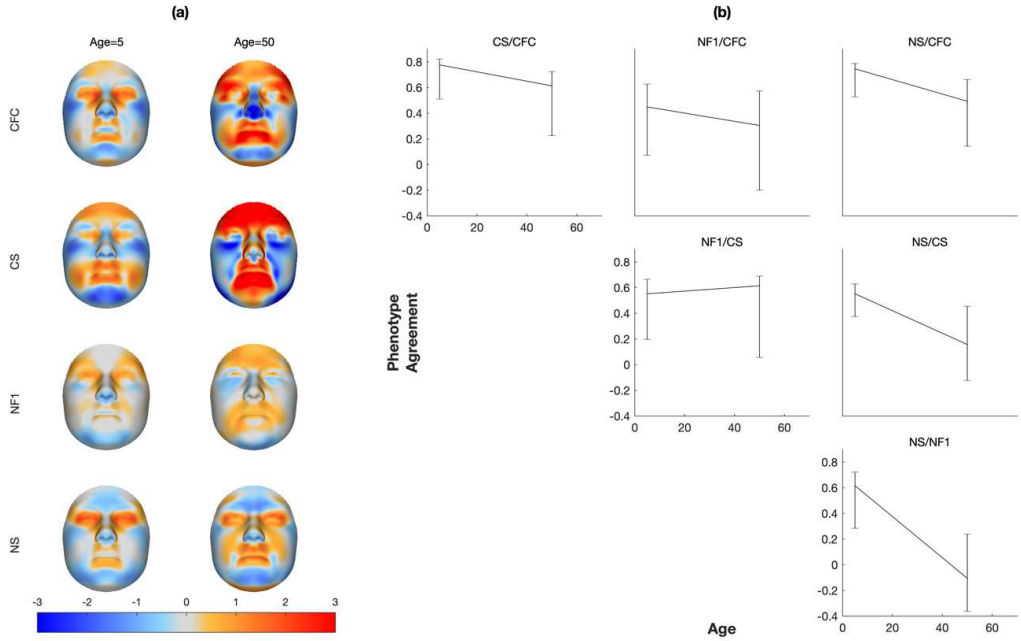

Supplementary Text Figure 3. Age-related changes in the typical phenotype and changes in the phenotype agreement statistic. Part (a) plots the expected signature at ages 5 and 50 predicted by a linear regression of the signatures in the direction normal to the facial surface (red indicates outward displacement, blue indicates inward displacement). Part (b) plots the expected changes in the phenotype agreement statistic as a result of the changes in the typical phenotype. 95% confidence intervals were calculated by resampling the data within each syndrome with replacement 1000 times, refitting the models and revaluating the expected signatures and phenotype agreement.

To assess how these changes affect the phenotype agreement statistic the phenotype agreement (cosine) between corresponding pairs of expected signatures was calculated. For example, to estimate the phenotype agreement between CS and NS at age 5 the cosine

between the expected signatures for CS at age 5 and for NS at age 5 was computed. Comparing the phenotype agreement at age 5 to age 50 reveals the general trend of how age-related changes in the phenotype influence the phenotype agreement statistic. These trends are plotted in Supplementary Text Figure 3 part (b). In general, the trend is for each syndrome to become more distinct (phenotype agreement decreases between all pairs of syndromes except NF1 and CS). The largest divergence is between NS and NF1 and NS and CS.

2.4 Age-related changes to severity differences

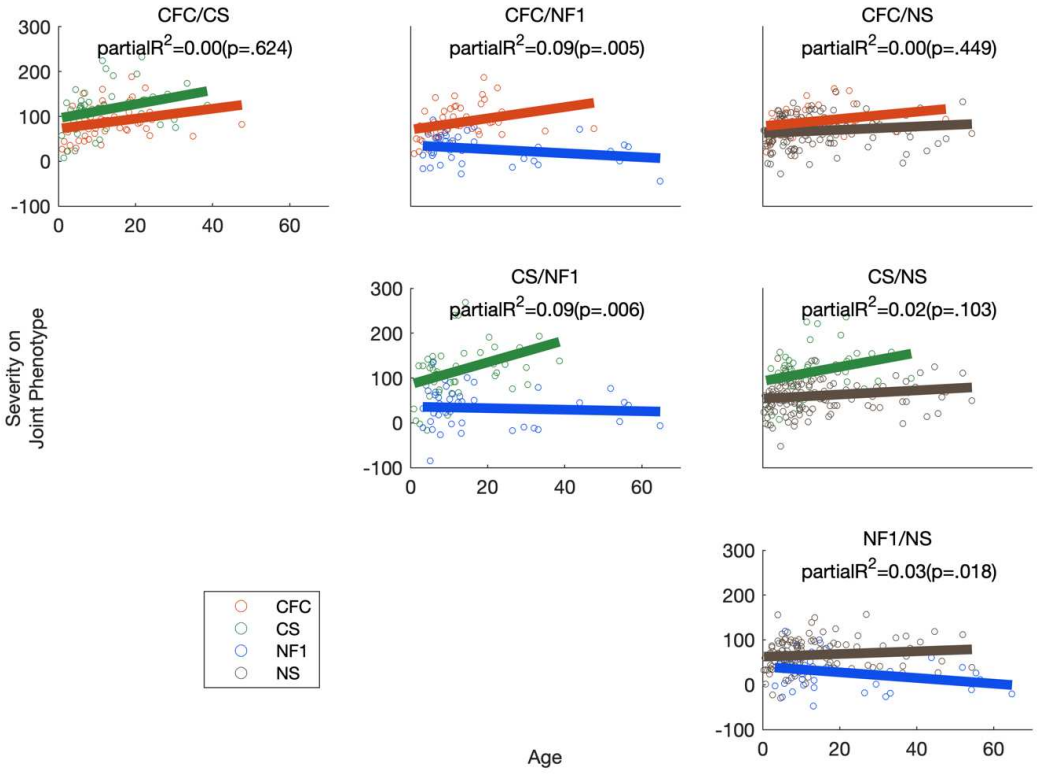

Supplementary Text Figure 4. Age-related changes to severity difference statistics. Each panel plots the severity scores along a combined phenotype for a particular pair of syndromes as a function of age. This is annotated with the linear regressions of age onto severity computed separately for each group. Text labels show the partial R^2 and p value associated with the interaction term of the corresponding general linear model (see text) and indicate the significance of the differences between regression slopes.

Severity difference is the difference between the central tendencies of the distributions of severity scores (expressed as Cohen's D statistic) of two syndromes. For calculating severity difference, severity is calculated with respect to the combined typical phenotype of both syndromes (estimated as the mean of the two mean signatures of the syndromes separately). This is done to jointly ordinate both syndromes on a common axis. To assess age-related changes in severity difference between each pair of syndromes we compare the slopes of linear regressions of these severity scores for each syndrome. This was done for each pair of syndromes by fitting a general linear model consisting of a main effect of syndrome (with two levels corresponding to the two syndromes in question), a main effect of age and a syndrome*age interaction. A significant interaction term indicates the slopes of the

regressions of age on severity differ between the two groups and that the difference in severity is either increasing or decreasing. Results are plotted in Supplementary Text Figure 4. For NF1 paired with CFC and CS and NF1 paired with NS the interaction is significant indicating that severity difference increases with age between these pairs of syndromes.

References

1 Shrimpton S, Daniels K, De Greef S, Tilotta F, Willems G, Vandermeulen D, Suetens P, Claes P. A spatially-dense regression study of facial form and tissue depth: Towards an interactive tool for craniofacial reconstruction. *Forensic Science International* 2014;**234**:103–10.

Supplementary Figures

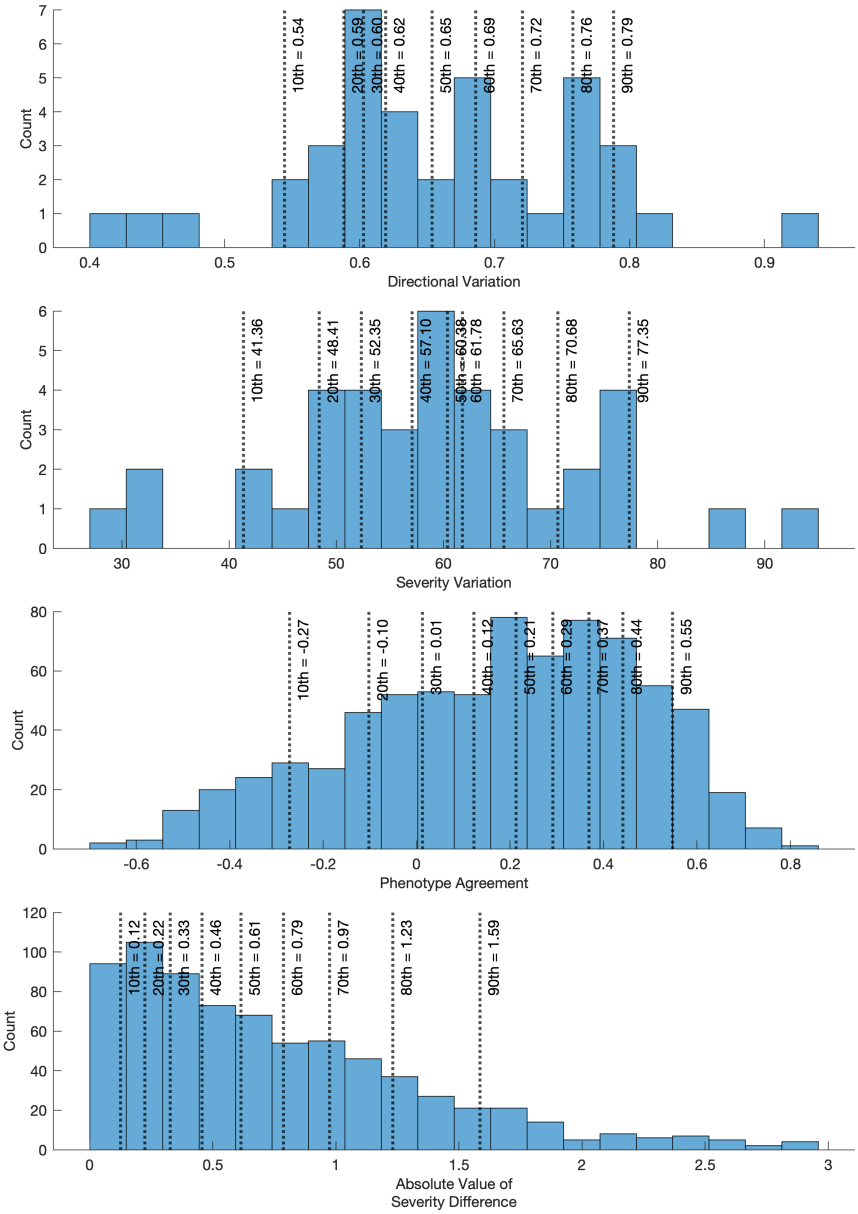

Supplementary Figure 1. Distributions of the directional variation, severity variation, phenotype agreement and severity difference statistics computed from the sample of disorders described in Supplementary Table 2.

Supplementary Tables

Supplementary Table 1. Image exclusion criteria. This shows the numbers remaining in each sample after each successive exclusion criterion was applied. Images were excluded due to 1) poor image quality including non-neutral facial expression, 2) missing data on age and sex or ethnicity, 3) failed image registration, 4) being a duplicate image of a patient already included in the analysis and 5) non-European ancestry. The final row, therefore, shows final numbers after all exclusion criteria were applied.

	CFC	CS	NF1	NS
INITIAL NUMBERS	76	77	94	174
POOR IMAGE QUALITY	62	60	87	161
MISSING DEMOGRAPHIC DATA	57	54	60	143
REGISTRATION FAILED	54	47	58	139
DUPLICATE PATIENT	54	46	55	132
NON-EUROPEAN ANCESTRY	51	46	42	129

Supplementary Table 2. Age, sex, clinical, and, where available, molecular diagnoses for each participant. Where available the molecular diagnosis at the gene, DNA and protein level as well as the variant's American College of Medical Genetics (ACMG) classification is reported.

Patient Study ID	Age (years)	Sex	Diagnosis	Molecular confirmation available	Gene	DNA	Protein	ACMG classification
CFC001	12.1	M	Cardiofaciocutaneous syndrome	Yes	MEK2			
CFC002	19.2	F	Cardiofaciocutaneous syndrome	Yes	BRAF			
CFC003	2.2	M	Cardiofaciocutaneous syndrome	No				
CFC004	2.5	F	Cardiofaciocutaneous syndrome	Yes	BRAF			
CFC005	1.5	F	Cardiofaciocutaneous syndrome	No				
CFC006	11.4	M	Cardiofaciocutaneous syndrome	Yes	BRAF			
CFC007	17.8	F	Cardiofaciocutaneous syndrome	No				
CFC008	9.4	M	Cardiofaciocutaneous syndrome	Yes	BRAF			
CFC009	3.7	F	Cardiofaciocutaneous syndrome	Yes	BRAF			
CFC010	4.6	F	Cardiofaciocutaneous syndrome	Yes	BRAF			
CFC011	7.8	F	Cardiofaciocutaneous syndrome	Yes	MEK1			
CFC012	4.4	M	Cardiofaciocutaneous syndrome	Yes	BRAF			
CFC013	19.0	F	Cardiofaciocutaneous syndrome	Yes	MEK1			
CFC014	6.5	F	Cardiofaciocutaneous syndrome	No				
CFC015	11.8	F	Cardiofaciocutaneous syndrome	Yes	BRAF			
CFC016	11.1	M	Cardiofaciocutaneous syndrome	No				
CFC017	15.9	F	Cardiofaciocutaneous syndrome	Yes	MEK1			
CFC018	6.9	F	Cardiofaciocutaneous syndrome	Yes	BRAF			
CFC019	7.9	M	Cardiofaciocutaneous syndrome	Yes	BRAF			
CFC020	8.8	F	Cardiofaciocutaneous syndrome	Yes	BRAF	c.770A>G	p.Gln257Arg	Pathogenic
CFC021	18.3	F	Cardiofaciocutaneous syndrome	No				
CFC022	20.7	M	Cardiofaciocutaneous syndrome	Yes	MAP2K1	c.389A>G	p.Tyr130Cys	Pathogenic
CFC023	22.8	M	Cardiofaciocutaneous syndrome	No				
CFC024	9.6	M	Cardiofaciocutaneous syndrome	No				

CFC025	6.1	M	Cardiofaciocutaneous syndrome	No				
CFC026	4.8	F	Cardiofaciocutaneous syndrome	Yes	BRAF	c.1787G>T	p.Gly596Val	Pathogenic
CFC027	24.3	F	Cardiofaciocutaneous syndrome	No				
CFC028	6.8	M	Cardiofaciocutaneous syndrome	Yes	BRAF			
CFC029	11.4	F	Cardiofaciocutaneous syndrome	Yes	BRAF	c.770A>G	p.Gln257Arg	Pathogenic
CFC030	11.9	M	Cardiofaciocutaneous syndrome	Yes	BRAF	c.1787G>T	p.Gly596Val	Pathogenic
CFC031	23.7	M	Cardiofaciocutaneous syndrome	Yes	BRAF			
CFC032	0.9	F	Cardiofaciocutaneous syndrome	Yes	BRAF	c.1497A>C	p.Lys499Asn	Pathogenic
CFC033	6.8	F	Cardiofaciocutaneous syndrome	Yes	BRAF	c.1406G>A	p.Gly469Glu	Pathogenic
CFC034	3.0	M	Cardiofaciocutaneous syndrome	Yes	BRAF			
CFC035	17.6	F	Cardiofaciocutaneous syndrome	Yes	BRAF			
CFC036	13.0	M	Cardiofaciocutaneous syndrome	Yes	MAP2K1	c.389A>G	p.Tyr130Cys	Pathogenic
CFC037	22.5	F	Cardiofaciocutaneous syndrome	Yes	BRAF			
CFC038	14.5	M	Cardiofaciocutaneous syndrome	Yes	MAP2K2	c.395G>A	p.Gly132Asp	Likely Pathogenic
CFC039	18.6	F	Cardiofaciocutaneous syndrome	No				
CFC040	8.4	M	Cardiofaciocutaneous syndrome	Yes	BRAF			
CFC041	4.5	M	Cardiofaciocutaneous syndrome	No				
CFC042	12.8	M	Cardiofaciocutaneous syndrome	Yes	BRAF			
CFC043	2.4	M	Cardiofaciocutaneous syndrome	No				
CFC044	11.1	F	Cardiofaciocutaneous syndrome	Yes	BRAF			
CFC045	10.4	F	Cardiofaciocutaneous syndrome	No				
CFC046	21.2	F	Cardiofaciocutaneous syndrome	No				
CFC047	23.7	F	Cardiofaciocutaneous syndrome	No				
CFC048	47.6	M	Cardiofaciocutaneous syndrome	Yes	BRAF			
CFC049	35.0	F	Cardiofaciocutaneous syndrome	Yes	BRAF	c.1787G>T	p.Gly596Val	Pathogenic
CFC050	2.5	F	Cardiofaciocutaneous syndrome	No				
CFC051	5.3	M	Cardiofaciocutaneous syndrome	No				

Costello001	0.9	F	Costello syndrome	Yes	HRAS			
Costello002	11.4	F	Costello syndrome	No				
Costello003	10.3	M	Costello syndrome	No				
Costello004	4.5	M	Costello syndrome	Yes	HRAS			
Costello005	12.3	F	Costello syndrome	Yes	HRAS			
Costello006	11.8	F	Costello syndrome	Yes	HRAS			
Costello007	26.4	M	Costello syndrome	Yes	HRAS			
Costello008	24.5	M	Costello syndrome	Yes	HRAS			
Costello009	22.4	M	Costello syndrome	Yes	HRAS			
Costello010	5.8	F	Costello syndrome	Yes	HRAS			
Costello011	21.8	F	Costello syndrome	Yes	HRAS			
Costello012	18.1	F	Costello syndrome	Yes	HRAS			
Costello013	21.5	M	Costello syndrome	Yes	HRAS			
Costello014	5.7	M	Costello syndrome	Yes	HRAS			
Costello015	21.9	F	Costello syndrome	Yes	HRAS			
Costello016	13.9	F	Costello syndrome	Yes	HRAS			
Costello017	11.6	F	Costello syndrome	Yes	HRAS			
Costello018	33.4	F	Costello syndrome	No				
Costello019	6.8	F	Costello syndrome	Yes	HRAS	c.34G>T	p.Gly12Cys	Pathogenic
Costello020	20.3	M	Costello syndrome	Yes	HRAS	c.34G>A	p.Gly12Ser	Pathogenic
Costello021	5.0	M	Costello syndrome	Yes	HRAS	c.34G>A	p.Gly12Ser	Pathogenic
Costello022	7.9	F	Costello syndrome	Yes	HRAS	c.37G>T	p.Gly13Cys	Pathogenic
Costello023	30.0	M	Costello syndrome	Yes	HRAS	c.34G>A	p.Gly12Ser	Pathogenic
Costello024	4.3	F	Costello syndrome	Yes	HRAS	c.37G>T	p.Gly13Cys	Pathogenic
Costello025	14.3	M	Costello syndrome	Yes	HRAS	c.34G>A	p.Gly12Ser	Pathogenic
Costello026	30.4	F	Costello syndrome	Yes	HRAS	c.34G>A	p.Gly12Ser	Pathogenic
Costello027	5.9	F	Costello syndrome	Yes	HRAS	c.34G>T	p.Gly12Cys	Pathogenic

Costello028	38.6	F	Costello syndrome	Yes	HRAS	c.34G>A	p.Gly12Ser	Pathogenic
Costello029	6.9	F	Costello syndrome	Yes	HRAS	c.34G>A	p.Gly12Ser	Pathogenic
Costello030	1.4	F	Costello syndrome	Yes	HRAS	c.34G>A	p.Gly12Ser	Pathogenic
Costello031	21.7	F	Costello syndrome	Yes	HRAS	c.34G>A	p.Gly12Ser	Pathogenic
Costello032	4.9	F	Costello syndrome	Yes	HRAS	c.34G>A	p.Gly12Ser	Pathogenic
Costello033	2.2	F	Costello syndrome	Yes	HRAS	c.34G>A	p.Gly12Ser	Pathogenic
Costello034	11.2	F	Costello syndrome	Yes	HRAS	c.34G>A	p.Gly12Ser	Pathogenic
Costello035	4.0	F	Costello syndrome	Yes	HRAS	c.34G>A	p.Gly12Ser	Pathogenic
Costello036	7.4	F	Costello syndrome	Yes	HRAS	c.34G>A	p.Gly12Ser	Pathogenic
Costello037	9.6	M	Costello syndrome	Yes	HRAS	c.34G>A	p.Gly12Ser	Pathogenic
Costello038	6.1	F	Costello syndrome	Yes	HRAS	c.34G>A	p.Gly12Ser	Pathogenic
Costello039	3.2	F	Costello syndrome	No				
Costello040	12.4	F	Costello syndrome	Yes	HRAS	c.34G>A	p.Gly12Ser	Pathogenic
Costello041	5.4	F	Costello syndrome	Yes	HRAS	c.34G>T	p.Gly12Cys	Pathogenic
Costello042	6.8	M	Costello syndrome	Yes	HRAS	c.34G>A	p.Gly12Ser	Pathogenic
Costello043	2.4	F	Costello syndrome	Yes	HRAS	c.37G>T	p.Gly13Cys	Pathogenic
Costello044	7.4	M	Costello syndrome	Yes	HRAS	c.34G>A	p.Gly12Ser	Pathogenic
Costello045	28.4	M	Costello syndrome	Yes	HRAS	c.34G>A	p.Gly12Ser	Pathogenic
Costello046	10.7	M	Costello syndrome	Yes	HRAS	c.37G>T	p.Gly13Cys	Pathogenic
NF001	13.4	M	Neurofibromatosis type 1	Yes	NF1	c.7954C>T	p.Gln2652Ter	Pathogenic
NF002	7.7	M	Neurofibromatosis type 1	Yes	NF1			
NF003	13.3	F	Neurofibromatosis type 1	No				
NF004	3.3	M	Neurofibromatosis type 1	No				
NF005	54.3	F	Neurofibromatosis type 1	No				
NF006	10.6	M	Neurofibromatosis type 1	No				
NF007	51.9	F	Neurofibromatosis type 1	No				
NF008	16.5	M	Neurofibromatosis type 1	Yes	NF1	c.1466A>G	p.Tyr489Cys	Pathogenic

NF009	10.2	M	Neurofibromatosis type 1	No				
NF010	12.8	F	Neurofibromatosis type 1	Yes	NF1	Deletion exons 39-45		Pathogenic
NF011	7.5	F	Neurofibromatosis type 1	No				
NF012	9.3	F	Neurofibromatosis type 1	No				
NF013	10.9	F	Neurofibromatosis type 1	No				
NF014	12.3	M	Neurofibromatosis type 1	No				
NF015	5.5	M	Neurofibromatosis type 1	Yes	NF1	c.1756_1759del	p.Thr586ValfsTer18	Pathogenic
NF016	7.3	F	Neurofibromatosis type 1	No				
NF017	5.8	F	Neurofibromatosis type 1	Yes	NF1	Microdeletion		Pathogenic
NF018	9.1	F	Neurofibromatosis type 1	Yes	NF1	c.3457_3460del	p.Leu1153fsMetfsTer 4	Pathogenic
NF019	13.2	M	Neurofibromatosis type 1	No				
NF020	4.6	F	Neurofibromatosis type 1	Yes	NF1	c.7031del	p.Asn2344IlefsTer31	Pathogenic
NF021	16.5	F	Neurofibromatosis type 1	Yes	NF1			
NF022	6.4	M	Neurofibromatosis type 1	No				
NF023	3.2	M	Neurofibromatosis type 1	No				
NF024	5.5	F	Neurofibromatosis type 1	No				
NF025	5.2	M	Neurofibromatosis type 1	No				
NF026	6.0	F	Neurofibromatosis type 1	Yes	NF1	c.3938_3942del	p.Asp1313AlafsTer4	Pathogenic
NF027	8.9	M	Neurofibromatosis type 1	No				
NF028	33.1	M	Neurofibromatosis type 1	No				
NF029	56.5	F	Neurofibromatosis type 1	No				
NF030	10.3	M	Neurofibromatosis type 1	No				
NF031	6.3	F	Neurofibromatosis type 1	No				
NF032	64.8	F	Neurofibromatosis type 1	No				
NF033	7.3	F	Neurofibromatosis type 1	No				
NF034	26.4	F	Neurofibromatosis type 1	Yes	NF1	c.1019_1020del	p.Ser340CysfsTer12	Pathogenic
NF035	55.4	F	Neurofibromatosis type 1	No				

NF036	43.8	F	Neurofibromatosis type 1	No				
NF037	32.0	F	Neurofibromatosis type 1	No				
NF038	33.1	M	Neurofibromatosis type 1	No				
NF039	14.7	M	Neurofibromatosis type 1	No				
NF040	29.4	M	Neurofibromatosis type 1	No				
NF041	5.7	F	Neurofibromatosis type 1	No				
NF042	5.1	M	Neurofibromatosis type 1	Yes	NF1	c.4105del	p.Tyr1369ThrfsTer16	Pathogenic
Noonan001	2.4	M	Noonan syndrome	No				
Noonan002	28.6	F	Noonan syndrome	Yes	PTPN11			
Noonan003	14.9	M	Noonan syndrome	Yes	RAF1			
Noonan004	5.0	F	Noonan syndrome	Yes	NRAS			
Noonan005	9.0	M	Noonan syndrome	No				
Noonan006	4.0	M	Noonan syndrome	No				
Noonan007	46.5	M	Noonan syndrome	No				
Noonan008	47.6	F	Noonan syndrome	Yes	PTPN11			
Noonan009	7.4	M	Noonan syndrome	No				
Noonan010	13.2	M	Noonan syndrome	Yes	PTPN11			
Noonan011	40.9	F	Noonan syndrome	Yes	PTPN11			
Noonan012	16.5	F	Noonan syndrome	No				
Noonan013	12.6	M	Noonan syndrome	No				
Noonan014	5.0	F	Noonan syndrome	No				
Noonan015	37.2	F	Noonan syndrome	No				
Noonan016	5.2	F	Noonan syndrome	No				
Noonan017	18.6	M	Noonan syndrome	No				
Noonan018	7.1	F	Noonan syndrome	No				
Noonan019	38.3	F	Noonan syndrome	No				
Noonan020	1.2	F	Noonan syndrome	Yes	PTPN11			

Noonan021	2.0	M	Noonan syndrome	No	
Noonan022	7.9	M	Noonan syndrome	No	
Noonan023	5.3	M	Noonan syndrome	No	
Noonan024	45.5	M	Noonan syndrome	No	
Noonan025	6.0	F	Noonan syndrome	Yes	PTPN11
Noonan026	7.6	M	Noonan syndrome	No	
Noonan027	8.3	M	Noonan syndrome	No	
Noonan028	6.3	M	Noonan syndrome	Yes	PTPN11
Noonan029	37.3	F	Noonan syndrome	Yes	PTPN11
Noonan030	7.2	M	Noonan syndrome	No	
Noonan031	5.1	M	Noonan syndrome	Yes	BRAF
Noonan032	0.8	M	Noonan syndrome	No	
Noonan033	19.0	F	Noonan syndrome	Yes	PTPN11
Noonan034	8.4	M	Noonan syndrome	No	
Noonan035	8.4	M	Noonan syndrome	No	
Noonan036	2.7	M	Noonan syndrome	Yes	PTPN11
Noonan037	5.9	F	Noonan syndrome	No	
Noonan038	5.6	F	Noonan syndrome	No	
Noonan039	11.8	F	Noonan syndrome	No	
Noonan040	23.1	M	Noonan syndrome	No	
Noonan041	17.5	M	Noonan syndrome	No	
Noonan042	28.6	F	Noonan syndrome	No	
Noonan043	10.1	M	Noonan syndrome	No	
Noonan044	11.2	F	Noonan syndrome	No	
Noonan045	37.8	M	Noonan syndrome	No	
Noonan046	2.5	F	Noonan syndrome	No	
Noonan047	8.7	F	Noonan syndrome	No	

Noonan048	42.6	M	Noonan syndrome	No	
Noonan049	0.6	M	Noonan syndrome	No	
Noonan050	13.5	F	Noonan syndrome	No	
Noonan051	16.0	F	Noonan syndrome	Yes	PTPN11
Noonan052	12.7	M	Noonan syndrome	Yes	PTPN11
Noonan053	4.6	M	Noonan syndrome	No	
Noonan054	10.0	F	Noonan syndrome	No	
Noonan055	4.5	M	Noonan syndrome	No	
Noonan056	29.5	M	Noonan syndrome	No	
Noonan057	16.0	M	Noonan syndrome	No	
Noonan058	8.2	M	Noonan syndrome	No	
Noonan059	2.6	M	Noonan syndrome	No	
Noonan060	44.6	F	Noonan syndrome	No	
Noonan061	19.5	M	Noonan syndrome	Yes	PTPN11
Noonan062	2.4	F	Noonan syndrome	Yes	PTPN11
Noonan063	4.5	M	Noonan syndrome	No	
Noonan064	5.7	M	Noonan syndrome	No	
Noonan065	10.0	F	Noonan syndrome	No	
Noonan066	7.4	M	Noonan syndrome	No	
Noonan067	7.4	M	Noonan syndrome	No	
Noonan068	1.8	F	Noonan syndrome	No	
Noonan069	39.7	M	Noonan syndrome	No	
Noonan070	9.4	M	Noonan syndrome	No	
Noonan071	2.0	F	Noonan syndrome	No	
Noonan072	1.9	M	Noonan syndrome	Yes	PTPN11
Noonan073	2.4	M	Noonan syndrome	Yes	PTPN11
Noonan074	1.7	M	Noonan syndrome	Yes	PTPN11

Noonan075	3.1	M	Noonan syndrome	No				
Noonan076	6.4	M	Noonan syndrome	No				
Noonan077	12.1	M	Noonan syndrome	Yes	PTPN11			
Noonan078	30.4	F	Noonan syndrome	Yes	SOS1			
Noonan079	0.8	F	Noonan syndrome	Yes	SOS1			
Noonan080	14.9	F	Noonan syndrome	Yes	PTPN11	c.922A>G	p.Asn308Asp	Pathogenic
Noonan081	18.4	M	Noonan syndrome	No				
Noonan082	6.5	M	Noonan syndrome	Yes	PTPN11	c.1472C>A	p.Pro491His	Pathogenic
Noonan083	5.9	F	Noonan syndrome	Yes	PTPN11	c.1510A>G	p.Met504Val	Pathogenic
Noonan084	5.5	F	Noonan syndrome	Yes	PTPN11	c.922A>G	p.Asn308Asp	Pathogenic
Noonan085	31.3	F	Noonan syndrome	Yes	PTPN11	c.922A>G	p.Asn308Asp	Pathogenic
Noonan086	17.5	M	Noonan syndrome	Yes	PTPN11	c.922A>G	p.Asn308Asp	Pathogenic
Noonan087	5.0	F	Noonan syndrome	No				
Noonan088	2.1	M	Noonan syndrome	No				
Noonan089	1.3	F	Noonan syndrome	Yes	PTPN11	c.802G>T	p.Gly268Cys	Pathogenic
Noonan090	19.3	M	Noonan syndrome	Yes	PTPN11			
Noonan091	51.9	F	Noonan syndrome	Yes	PTPN11	c.317A>C	p.Asp106Ala	Pathogenic
Noonan092	36.4	F	Noonan syndrome	No				
Noonan093	21.7	F	Noonan syndrome	No				
Noonan094	17.2	F	Noonan syndrome	Yes	PTPN11	c.417G>C	p.Glu139Asp	Pathogenic
Noonan095	8.3	M	Noonan syndrome	Yes	RAF1			
Noonan096	13.5	F	Noonan syndrome	Yes	PTPN11			
Noonan097	18.9	M	Noonan syndrome	Yes	PTPN11			
Noonan098	3.8	M	Noonan syndrome	Yes	PTPN11	c.923A>G	p.Asn308Ser	Pathogenic
Noonan099	9.6	M	Noonan syndrome	Yes	PTPN11			
Noonan100	15.3	F	Noonan syndrome	Yes	PTPN11	c.1403C>T	p.Thr468Met	Pathogenic
Noonan101	3.9	M	Noonan syndrome	Yes	PTPN11			

Noonan102	0.3	F	Noonan syndrome	Yes	PTPN11			
Noonan103	34.6	F	Noonan syndrome	No				
Noonan104	8.6	M	Noonan syndrome	Yes	PTPN11	c.1471C>T	p.Pro491Ser	Pathogenic
Noonan105	9.2	F	Noonan syndrome	No				
Noonan106	16.4	F	Noonan syndrome	Yes	PTPN11			
Noonan107	15.6	M	Noonan syndrome	Yes	PTPN11			
Noonan108	10.3	M	Noonan syndrome	Yes	PTPN11			
Noonan109	6.4	M	Noonan syndrome	Yes	PTPN11			
Noonan110	27.3	F	Noonan syndrome	Yes	PTPN11			
Noonan111	9.6	M	Noonan syndrome	Yes	SOS1	c.1654A>G	p.Arg552Gly	Pathogenic
Noonan112	36.3	F	Noonan syndrome	Yes	SOS1	c.1654A>G	p.Arg552Gly	Pathogenic
Noonan113	26.9	F	Noonan syndrome	No				
Noonan114	24.8	M	Noonan syndrome	Yes	SOS1			
Noonan115	24.5	F	Noonan syndrome	Yes	RAF1			
Noonan116	12.2	M	Noonan syndrome	Yes	PTPN11			
Noonan117	15.7	M	Noonan syndrome	Yes	SOS1			
Noonan118	4.2	M	Noonan syndrome	Yes	PTPN11			
Noonan119	9.7	F	Noonan syndrome	Yes	SHOC2	c.4A>G	p.Ser2Gly	Pathogenic
Noonan120	9.7	F	Noonan syndrome	Yes	SHOC2	c.4A>G	p.Ser2Gly	Pathogenic
Noonan121	17.7	F	Noonan syndrome	Yes	SOS1	c.1859A>G	p.Asp.620Gly	Likely Pathogenic
Noonan122	54.3	F	Noonan syndrome	Yes	SOS1	c.1310T>C	p.Ile437Thr	Pathogenic
Noonan123	3.9	F	Noonan syndrome	Yes	PTPN11	c.184T>G	p.Tyr62Asp	Pathogenic
Noonan124	4.7	M	Noonan syndrome	Yes	CBL	c.1477C>T	p.Leu493Phe	Uncertain Significance
Noonan125	8.0	F	Noonan syndrome	Yes	PTPN11	c.1403C>T	p.Thr468Met	Pathogenic
Noonan126	6.7	M	Noonan syndrome	Yes	PTPN11	c.1403C>T	p.Thr468Met	Pathogenic
Noonan127	13.0	M	Noonan syndrome	Yes	PTPN11	c.1403C>T	p.Thr468Met	Pathogenic
Noonan128	12.1	M	Noonan syndrome	Yes	SOS1	c.1310T>C	p.Ile437Thr	Pathogenic

Noonan129	5.8	M	Noonan syndrome	No

Supplementary Table 3. Samples used to calculate the distributions of the directional variation, severity variation, phenotype agreement and severity difference statistics shown in Supplementary Figure 1. The sample contains only patients of European ancestry. It is known that in the portion of the data coming from the Peter Hammond collection images of the same participant, taken at multiple times, were not always linked by a consistent subject ID. As such this data (although not the RASopathy sample) may contain duplicate images of the same subjects.

Condition	N(Female)	Age Median (IQR)
22q11.2 Del	146(71)	9.25(7.70)
5p Del Cri du Chat	61(34)	13.03(15.90)
Achondroplasia	46(29)	16.28(23.17)
Alstrom	40(19)	23.85(17.60)
Angelman	100(49)	8.15(8.57)
Bardet Biedl	81(40)	24.50(22.92)
CHARGE	89(48)	13.16(11.23)
Cleft Lip Palate	76(27)	9.39(6.12)
Cockayne	33(15)	10.64(9.58)
Cohen	27(15)	18.58(15.75)
Cornelia de Lange	169(91)	11.03(11.59)
Trisomy 21	86(47)	19.71(17.00)
Ectodermal Dysplasia	59(16)	9.80(10.00)
Ehlers Danlos	86(73)	28.42(32.40)
Fabry	35(15)	35.80(26.10)
Fibrodysplasia Ossificans Progressiva	50(28)	18.90(11.90)
Fragile X	62(20)	14.95(17.40)
Galactosemia	38(21)	18.65(18.40)
Jacobsen	53(33)	10.60(9.80)
Joubert	46(21)	8.14(8.90)
Klinefelter	39(0)	16.65(8.60)
Loeys Dietz	62(38)	19.94(21.47)
Marfan	84(54)	20.79(22.82)
Mucopolysaccharidosis	47(22)	18.65(12.42)
Pallister Killian	23(7)	7.22(7.40)
Phelan McDermid	37(16)	9.46(11.20)
Pitt Hopkins	25(15)	8.56(8.41)
Prader Willi	87(43)	15.40(21.70)
Pseudoachondroplasia	25(11)	24.42(26.75)
Rett	45(43)	11.30(8.70)
Rubinstein Taybi	57(30)	9.75(12.40)
Russell Silver	31(8)	7.11(5.43)
Smith Magenis	112(60)	12.40(11.50)
Sotos	37(18)	15.00(11.67)
Stickler	25(16)	20.25(27.08)
Trisomy 18	20(17)	4.70(14.43)
Turner	76(76)	17.84(25.40)
Williams	198(93)	13.50(19.70)
Wolf Hirschhorn	132(73)	7.40(8.50)

Supplementary Table 4. Percentiles of the directional variation, severity variation, phenotype agreement and severity difference statistics computed from the sample of disorders described in Supplementary Table 1.

Percentile	Directional Variation	Severity Variation	Phenotype Agreement	Absolute Value of Severity Difference
1	0.404999599	28.92045205	-0.52858594	0.016847016
2	0.41691339	29.69415697	-0.485725252	0.021956743
3	0.433507598	30.7718174	-0.445224629	0.031892556
4	0.448709565	31.80459449	-0.425861184	0.043587749
5	0.456254203	32.59051316	-0.400588616	0.050268766
6	0.46379884	33.37643182	-0.353876627	0.070652875
7	0.484689684	35.45224114	-0.339692853	0.091097979
8	0.514864846	38.42536568	-0.318528068	0.101799021
9	0.544270101	41.32330631	-0.301932579	0.112765583
10	0.544418946	41.36425794	-0.272389088	0.124896126
11	0.544567791	41.40520958	-0.246851531	0.130653152
12	0.549794209	42.42365033	-0.233848096	0.141251409
13	0.560944463	44.58249504	-0.206593641	0.157235544
14	0.572094716	46.74133976	-0.189189947	0.160257308
15	0.574371473	47.32777583	-0.175639719	0.1691268
16	0.575634115	47.73450807	-0.153246915	0.179394117
17	0.577545298	48.04556819	-0.137678098	0.190353735
18	0.58075356	48.16528408	-0.127254361	0.200124617
19	0.583961823	48.28499997	-0.119635721	0.214921595
20	0.58826769	48.40684978	-0.102030942	0.224104632
21	0.592902839	48.52933976	-0.092151505	0.235993994
22	0.596618194	48.62921088	-0.077809264	0.247289468
23	0.596769349	48.64143392	-0.06651491	0.257490421
24	0.596920503	48.65365696	-0.054163178	0.272063147
25	0.597867259	49.46089825	-0.043292773	0.279704625
26	0.599259551	50.71334978	-0.025370132	0.287243384
27	0.600590289	51.87781068	-0.014045098	0.298807062
28	0.601182369	51.98638412	-0.006242112	0.308058208
29	0.601774449	52.09495756	0.000322494	0.316834715
30	0.60286507	52.34537563	0.012634634	0.32727041
31	0.604429303	52.7305461	0.024875947	0.33640357
32	0.605993536	53.11571657	0.034724832	0.351132668
33	0.608881173	53.41453815	0.042863877	0.368565002
34	0.611840345	53.70869223	0.05612422	0.375131549
35	0.613835775	53.97945631	0.068660436	0.39415268
36	0.61428922	54.2127964	0.07463783	0.404921783
37	0.614742664	54.44613649	0.086679864	0.420028861
38	0.615680065	55.31488247	0.096996213	0.432109909
39	0.616723331	56.32262349	0.113122373	0.445920564
40	0.619354165	57.09764799	0.12264453	0.456350037
41	0.626588942	57.19779458	0.135664084	0.470895852
42	0.633823718	57.29794117	0.147722802	0.494885555
43	0.636096646	57.56437	0.156544542	0.514116247
44	0.636164307	57.90470205	0.16620765	0.532014946
45	0.636452491	58.2750225	0.1709629	0.54865238

46	0.638240232	58.84926406	0.180212157	0.565157187
47	0.640027973	59.42350561	0.192127323	0.569425485
48	0.643633462	59.82844935	0.198317709	0.580330584
49	0.648643577	60.10257205	0.206122841	0.597527253
50	0.653653691	60.37669475	0.212676274	0.614732872
51	0.653922338	60.39669513	0.219226314	0.630485583
52	0.654190984	60.4166955	0.223379421	0.643380665
53	0.657222874	60.48027156	0.228085102	0.653735383
54	0.663830725	60.60023969	0.23749279	0.673943029
55	0.670438576	60.72020782	0.251534632	0.683933297
56	0.674979863	60.75346087	0.263092644	0.699428863
57	0.679217244	60.7739617	0.27420552	0.715200795
58	0.68265319	60.92039418	0.278728141	0.74044451
59	0.684285909	61.35017287	0.284528862	0.758677151
60	0.685918627	61.77995156	0.29123443	0.787295617
61	0.686591799	62.11642507	0.298745538	0.81105458
62	0.686934092	62.42072439	0.305713738	0.844772068
63	0.687565368	62.68240575	0.319709285	0.860189119
64	0.689517707	62.74926218	0.325550635	0.871315338
65	0.691470046	62.81611861	0.331809459	0.885007217
66	0.696886125	63.17359125	0.335124464	0.898300364
67	0.704467042	63.71269902	0.34129593	0.918053963
68	0.711883745	64.25939104	0.350479885	0.933788091
69	0.716262492	64.94639162	0.359060528	0.946742761
70	0.720641238	65.63339219	0.368632278	0.974973159
71	0.725311118	66.09200876	0.375512234	0.991180644
72	0.730287454	66.31022111	0.382475387	1.00885399
73	0.73526379	66.52843345	0.390684364	1.043605521
74	0.741733141	66.82796853	0.396356167	1.079276615
75	0.74832691	67.13428051	0.40249041	1.101180428
76	0.752678911	67.48566791	0.409013986	1.114756503
77	0.753027756	67.91754717	0.420882268	1.141143105
78	0.753376602	68.34942642	0.426383015	1.162120011
79	0.755461418	69.43105669	0.434304392	1.184544405
80	0.757994227	70.68036465	0.441321488	1.230923428
81	0.760371186	71.87864921	0.450976424	1.257246158
82	0.762228645	72.90685582	0.45956105	1.289676885
83	0.764086105	73.93506243	0.472471772	1.307930182
84	0.765616672	74.85288998	0.482581664	1.354532256
85	0.766983794	75.71552799	0.491598671	1.382650721
86	0.768777103	76.49413663	0.500678837	1.429282333
87	0.774299547	76.53748826	0.512852073	1.462859138
88	0.779821992	76.5808399	0.528063164	1.501453554
89	0.7843843	76.86151901	0.539582697	1.528268688
90	0.788123635	77.34562167	0.547404315	1.585376202
91	0.79186297	77.82972433	0.559359602	1.645946186
92	0.794951644	77.86422628	0.566901366	1.704244215
93	0.798023194	77.88689663	0.578600136	1.768111948
94	0.803268253	79.52813461	0.593754561	1.843759203

95	0.811637728	83.49606358	0.609212164	1.926300134
96	0.820007203	87.46399254	0.618909216	2.098060149
97	0.857372891	89.70020562	0.646134562	2.250903694
98	0.900010617	91.62156127	0.672879985	2.414908545
99	0.930622318	93.00099609	0.726058879	2.567521846
100	0.930622318	93.00099609	0.858244726	2.957309988